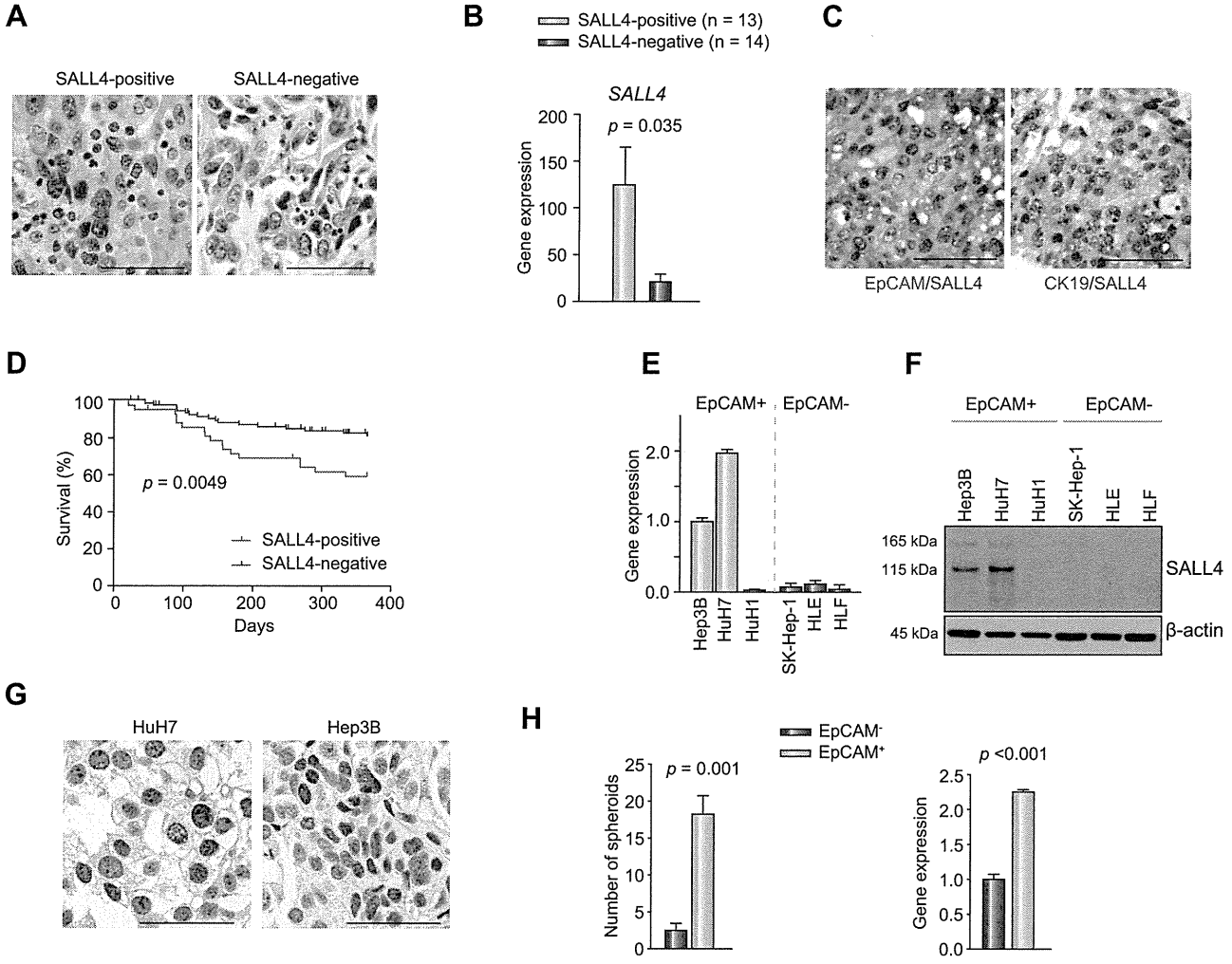

Fig. 2. *SALL4* expression in human primary HCCs and cell lines. (A) Representative images of SALL4-positive and -negative HCC immunostaining (scale bar, 100 μm). (B) Gene expression of *SALL4* in SALL4-positive (n = 13) and -negative HCCs (n = 14) as shown by IHC (mean ± SD). (C) Double color IHC analysis of HCC stained with anti-SALL4 and anti-EpCAM or anti-CK19 antibodies (scale bar, 100 μm). (D) Kaplan-Meier survival analysis with Log-rank. Recurrence-free survival of SALL4-positive (n = 43) and -negative (n = 101) HCCs was analyzed. (E) *SALL4* expression in EpCAM$^+$ (Hep3B, HuH7, and HuH1) and EpCAM$^-$ (SK-Hep-1, HLE, and HLF) HCC cell lines evaluated by qRT-PCR. (F) SALL4 expression in EpCAM$^+$ and EpCAM$^-$ HCC cell lines evaluated by Western blotting. (G) IHC analysis of SALL4 expression in subcutaneous tumors obtained from EpCAM$^+$ (HuH7 and Hep3B) HCC cell lines xenografted in NOD/SCID mice. (H) Spheroid formation capacity of sorted EpCAM$^+$ and EpCAM$^-$ cells obtained from a primary HCC. Number of spheroids obtained from 2000 sorted cells is indicated (n = 3, mean ± SD). Gene expression of *SALL4* in sorted EpCAM$^+$ and EpCAM$^-$ cells obtained from a primary HCC (n = 3, mean ± SD). (This figure appears in colour on the web.)

SALL4-positive HCCs were associated with expression of the hepatic stem cell markers EpCAM and CK19. Co-expression of SALL4, EpCAM, and CK19 was confirmed by double color IHC analysis (Fig. 2C). Evaluation of the survival outcome of these surgically resected HCC cases by Kaplan-Meier survival analysis indicated that SALL4-positive HCCs were associated with significantly lower recurrence-free survival outcomes within one year compared with SALL4-negative HCCs ($p = 0.0049$) (Fig. 2D).

Because SALL4 expression was positively correlated with EpCAM and AFP expression in primary HCC cases, we evaluated the expression of SALL4 in EpCAM$^+$ AFP$^+$ and EpCAM$^-$ AFP$^-$ HCC cell lines. Consistent with the primary HCC data, two of three EpCAM$^+$ AFP$^+$ HCC cell lines (Hep3B and HuH7) abundantly expressed SALL4, as shown by qRT-PCR (Fig. 2E) and Western blotting (Fig. 2F). We identified the expression of two isoforms of SALL4 proteins with molecular weights of 165 kDa (SALL4A) and 115 kDa (SALL4B), and SALL4B was found to be the dominant endogenous isoform in HCC cell lines. All EpCAM$^-$ AFP$^-$ HCC cell lines (SK-Hep-1, HLE, and HLF) and one EpCAM$^+$ AFP$^+$ cell line (HuH1) did not express SALL4. Nuclear accumulation of SALL4 in Hep3B and HuH7 cells was confirmed by IHC using subcutaneous tumors developed in xenotransplanted NOD/SCID mice (Fig. 2G). We further evaluated the expression of *EPCAM* and *SALL4* using single cell suspensions derived from a surgically resected primary HCC. EpCAM$^+$ and EpCAM$^-$ cells were separated by magnetic beads, and we revealed a strong spheroid formation capacity of sorted EpCAM$^+$ cells compared with EpCAM$^-$ cells (Fig. 2H, left panel). Interestingly, when comparing the expression of *SALL4* in these sorted cells, we identified a high expression of *SALL4* in sorted EpCAM$^+$ cells compared with EpCAM$^-$ cells (Fig. 2H, right panel), indicating that SALL4 is activated in EpCAM$^+$ liver CSCs.

Table 1. Clinicopathological characteristics of SALL4-positive and -negative HCC cases used for IHC analyses.

Parameters	SALL4-positive (n = 43)	SALL4-negative (n = 101)	*p* value*
Age (yr, mean ± SE)	60.8 ± 1.8	64.6 ± 1.0	0.13
Sex (male/female)	27/16	70/18	0.06
Etiology (HBV/HCV/B + C/other)	21/14/0/8	20/63/3/15	0.0014
Liver cirrhosis (yes/no)	21/22	61/40	0.27
AFP (ng/ml, mean ± SE)	13,701 ± 9292	175.5 ± 55.0	<0.0001
Histological grade**			
I-II	3	18	
II-III	33	68	
III-IV	7	15	0.24
Tumor size (<3 cm/>3 cm)	17/26	57/44	0.071
EpCAM (positive/negative)	27/16	29/72	0.0002
CK19 (positive/negative)	12/31	12/89	0.027

*Mann-Whitney U-test or χ^2 test.
**Edmondson-Steiner.

SALL4 regulates stemness of HpSC-HCC

To explore the role of SALL4 in HpSC-HCC, we evaluated the effect of its overexpression in HuH1 cells which showed little expression of SALL4 irrespective of EpCAM$^+$ and AFP$^+$ HpSC-HCC phenotype. We transfected plasmid constructs encoding SALL4 (pCMV6-SALL4) or control (pCMV7), and we similarly identified the expression of two isoforms by using this construct (Fig. 3A). Evaluation of the subcellular localization of GFP-tagged SALL4 (pCMV6-SALL4-GFP) showed that it could be detected in both the cytoplasm and nucleus (Fig. 3B). We observed strong up-regulation of the hepatic stem cell marker *KRT19*, modest up-regulation of *EPCAM* and *CD44*, and down-regulation of the mature hepatocyte marker *ALB* in HuH1 cells transfected with pCMV6-SALL4 compared with the control (Fig. 3C). Up-regulation of CK19 by SALL4 overexpression was also confirmed at the protein level by IF analysis (Fig. 3D). Phenotypically, SALL4 overexpression in HuH1 cells resulted in the significant activation of spheroid formation and invasion capacities with activation of *SNAI1*, which induces epithelial-mesenchymal transition, compared with the control (Fig. 3E and F, Supplementary Fig. 1A).

We further investigated the effect of SALL4 knockdown in HuH7 cells, which intrinsically expressed high levels of SALL4. Expression of *SALL4* was decreased to 50% in HuH7 cells transfected with SALL4 sh-RNA compared with the control when evaluated by qRT-PCR (Fig. 4A). However, the reduction of SALL4 protein was more evident when evaluated by Western blotting, suggesting that this sh-RNA construct might work at the translational as well as the transcriptional level (Fig. 4B). Knock down of *SALL4* resulted in a compromised invasion capacity and spheroid formation capacity with decreased expression of *EPCAM* and *CD44* in HuH7 cells (Fig. 4C and D, Supplementary Fig. 1B and C).

SALL4 and HDAC activity in HpSC-HCC

The above data suggested that SALL4 is a good target and biomarker for the diagnosis and treatment of HpSC-HCCs. However, it is difficult to directly target SALL4 as no studies have investigated the inhibition of its transcription using chemical or other approaches [21]. We therefore re-investigated the interaction networks associated with *SALL4*, and found that SALL4 activation appeared to induce epigenetic modification (Fig. 1B). In particular, a recent study suggested that SALL4 forms a nucleosome remodeling and deacetylase (NuRD) complex with HDACs and potentially regulates HDAC activity [22]. We therefore confirmed that *SALL4* knock down resulted in the reduced activity of total HDAC in HuH7 cells (Fig. 4E). We also evaluated the effect of the overexpression of SALL4 in HuH1 and HLE cells, which do not express SALL4 endogenously, and SALL4 overexpression was found to result in a modest increase of HDAC activity and mild enhancement of chemosensitivity to an HDAC inhibitor SBHA in both cell lines (Supplementary Fig. 2A and B). We further investigated HDAC activity in two SALL4-positive (Hep3B, HuH7) and two SALL4-negative (HLE, HLF) HCC cell lines. Interestingly, high HDAC activities were detected in SALL4-positive compared with SALL4-negative HCC cell lines (Fig. 4F). The HDAC inhibitor SBHA was found to inhibit proliferation of SALL4-positive HCC cell lines at a concentration of 10 μM. By contrast, SBHA had little effect on the proliferation of SALL4-negative HCC cell lines at this concentration (Fig. 4G). SBHA treatment suppressed the expression of SALL4 gene/protein expression in SALL4-positive HuH7 and Hep3B cell lines (Supplementary Fig. 3A and B). We further investigated the effect of SAHA, an additional HDAC inhibitor, in these HCC cell lines, and SAHA was found to more efficiently suppress the cell proliferation of SALL4-positive cell lines compared with SALL4-negative cell lines (Supplementary Fig. 3C).

Taken together, our data suggest a pivotal role for the transcription factor SALL4 in regulating the stemness of HpSC-HCC. SALL4 was detected in HpSC-HCCs with poor prognosis, and inactivation of SALL4 resulted in a reduced invasion/spheroid formation capacity and decreased expression of hepatic stem cell markers. The HDAC inhibitors inhibited proliferation of SALL4-positive HCC cell lines with a reduction of SALL4 gene/protein expression, suggesting their potential in the treatment of SALL4-positive HpSC-HCC.

Discussion

Stemness traits in cancer cells are currently of great interest because they may explain the clinical outcome of patients according to the malignant nature of their tumor. Recently, we

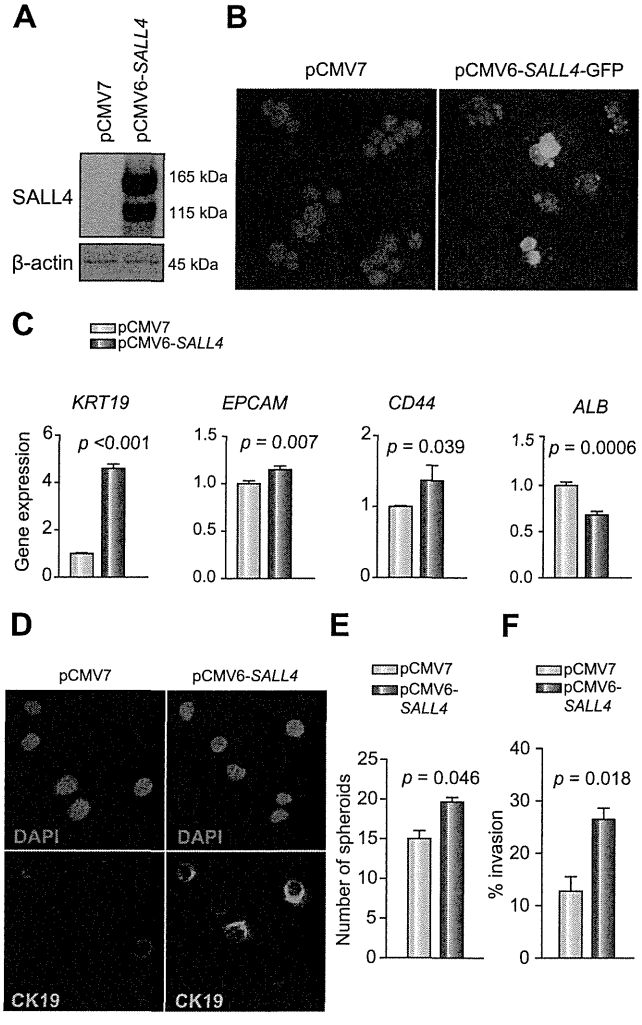

Fig. 3. Effect of SALL4 overexpression. (A) Western blots of cell lysates with anti-SALL4 antibodies. HuH1 cells were transfected with pCMV7 or pCMV6-*SALL4* and incubated for 72 h. (B) IF analysis of HuH1 cells transfected with pCMV7 or pCMV6-*SALL4* and incubated for 72 h. (C) qRT-PCR analysis of *KRT19*, *EPCAM*, *CD44*, and *ALB* in HuH1 cells transfected with pCMV7 or pCMV6-*SALL4* and incubated for 48 h. (D) IF analysis of HuH1 cells transfected with pCMV7 or pCMV6-*SALL4*, incubated for 72 h and stained with anti-CK19 antibodies, evaluated by the confocal laser scanning microscopy. (E) Spheroid formation assay of HuH1 cells transfected with pCMV7 or pCMV6-*SALL4*. Number of spheroids obtained from 2000 cells is indicated (n = 3, mean ± SD). (F) Invasion assay of HuH1 cells transfected with pCMV7 or pCMV6-*SALL4* (n = 3, mean ± SD). (This figure appears in colour on the web.)

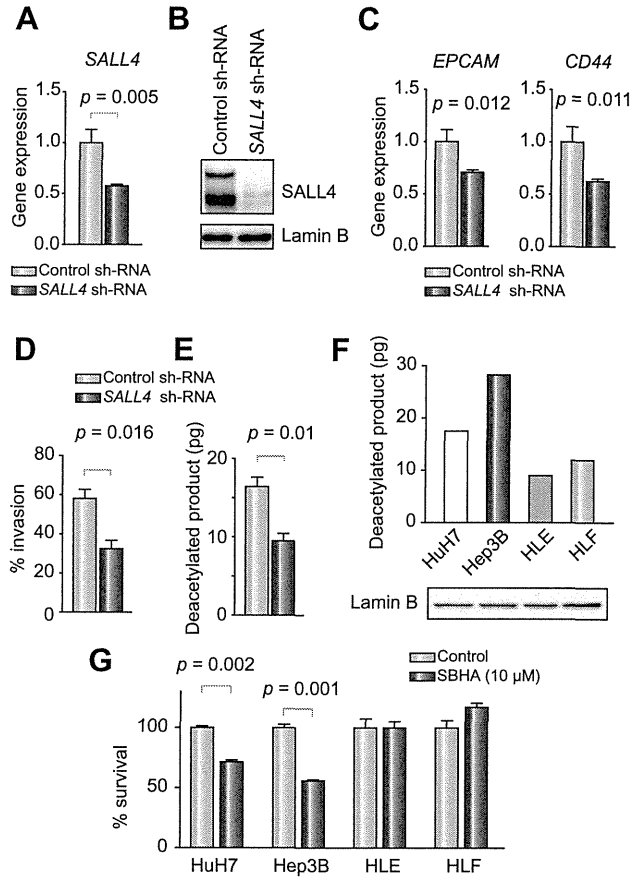

Fig. 4. Effect of *SALL4* knockdown and HDAC activity. (A) qRT-PCR analysis of *SALL4* in HuH7 cells transfected with control or *SALL4* sh-RNAs (n = 3, mean ± SD). (B) Western blots of lysates obtained from HuH7 cells transfected with control or *SALL4* sh-RNAs with anti-SALL4 antibodies. (C) qRT-PCR analysis of *EPCAM* and *CD44* in HuH7 cells transfected with control or *SALL4* sh-RNAs (n = 3, mean ± SD). (D) Invasion assay of HuH7 cells transfected with control or *SALL4* sh-RNAs (n = 3, mean ± SD). (E) HDAC activity of nuclear extracts obtained from HuH7 cells transfected with control or *SALL4* sh-RNAs. (F) HDAC activity of nuclear extracts obtained from each cell line. HDAC activity was measured in duplicate and average amounts of deacetylated products are indicated (upper panel). Lamin B included in the nuclear extracts loaded for HDAC activity assays was measured by Western blotting (lower panel). (G) Cell proliferation assay of HCC cell lines. Each cell line was treated with control DMSO or 10 μM SBHA and cultured for 72 h (n = 4, mean ± SD).

proposed an HCC classification system based on the stem/maturation status of the tumor by EpCAM and AFP expression status [8]. These HCC subtypes showed distinct gene expression patterns with features resembling particular stages of liver lineages. Among them, HpSC-HCC was characterized by a highly invasive nature, chemoresistance to fluorouracil, and poor prognosis after radical resection, warranting the development of a novel therapeutic approach against this HCC subtype [9].

In this study, we showed that the transcription factor SALL4 was activated in HpSC-HCC and that SALL4 might regulate HCC stemness, as characterized by the activation of EpCAM, CK19, and CD44 with highly tumorigenic and invasive natures. Furthermore, we identified that SALL4-positive HCC cell lines tended to show high HDAC activity and chemosensitivity to the HDAC inhibitors SBHA and SAHA. This study reveals for the first time the utility of SBHA for the treatment of HCC with stem cell features.

SALL4 is a zinc finger transcription factor originally cloned based on sequence homology to *Drosophila sal* [11]. *SALL4* mutations are associated with the Okihiro syndrome, a human disease involving multiple organ defects [23,24]. SALL4 plays a fundamental role in the maintenance of embryonic stem cells, potentially through interaction with Oct4, Sox2, and Nanog [25–30]. Furthermore, knockdown of SALL4 significantly reduces the efficiency of induced pluripotent stem cell generation [31]. *SALL4* is also expressed in hematopoietic stem cells and leukemia cells, where it regulates their maintenance [14,32]. SALL4 is known to encode two isoforms (SALL4A and SALL4B), and a recent study

suggested the important role of SALL4B on maintaining the stemness of embryonic stem cells [25]. Interestingly, our data indicated that SALL4B is also a dominant form in HpSC-HCC cell lines. It is unclear how SALL4 isoform expression is regulated in cancer, and future studies are required to explore the mechanisms of SALL4 isoform regulation.

In the liver, SALL4 is expressed in fetal hepatic stem/progenitors but not in adult hepatocytes, and a mouse study demonstrated that inhibition of SALL4 in hepatic stem/progenitors contributes to their differentiation [33]. Interestingly, recent studies indicated that AFP-producing gastric cancer expresses SALL4, suggesting that SALL4 might play a role in the hepatoid differentiation of gastric cancer [34]. Consistently, our data indicated a positive correlation between *SALL4*, *AFP*, and *EPCAM* expression in two independent HCC cohorts. Strikingly, SALL4 was recently shown to be expressed in a subset of human liver cancers with poor prognoses, while modification of SALL4 expression resulted in the alteration of cell proliferation *in vitro* and tumor growth *in vivo*, consistent with our current study [35]. A recent study reported the expression of SALL4 in 46% of HCC cases, which is almost comparable to our present study [36]. Furthermore, a very recent study of two independent large cohorts demonstrated that SALL4 is a marker for a progenitor subclass of HCC with an aggressive phenotype [37]. It is still unclear how SALL4 expression is regulated and which target genes are directly activated by SALL4 binding. Future studies using next generation sequencing are required to fully understand the mechanisms of SALL4 regulation of HCC stemness.

In this study, we demonstrated that SALL4-positive HCC cell lines have high HDAC activity and chemosensitivity against the HDAC inhibitors SBHA and SAHA compared with SALL4-negative HCC cell lines. SALL4 was recently found to directly connect with the epigenetic modulator NuRD complex [22], thereby possibly affecting the histone modification associated with stemness. The NuRD complex is a multiunit chromatin remodeling complex containing chromodomain-helicase-DNA-binding proteins and HDACs that regulate histone deacetylation [38]. Its role in cancer is still controversial, while its function in HCC has not yet been determined.

Our data suggest that SALL4 plays a role in controlling HDAC activity and contributing to the maintenance of HCC with stem cell features. Consistently, HDAC inhibitors might be useful for the eradication of SALL4-positive HCC cells through their inhibitory effects on histone deacetylation by NuRD [39]. Encouragingly, a recent study demonstrated the utility of a SALL4-binding peptide to inhibit its binding to phosphatase and tensin homolog deleted on chromosome 10 (PTEN) through interaction with HDAC, thereby targeting leukemia cells [21]. Further studies are required to understand the relationship between SALL4, the NuRD complex, and the maintenance of stemness in HCC.

Financial support

This study was supported by a Grant-in-Aid from the Ministry of Education, Culture, Sports, Science and Technology, Japan (23590967), a grant from the Japanese Society of Gastroenterology, a grant from the Ministry of Health, Labour and Welfare, and a grant from the National Cancer Center Research and Development Fund (23-B-5), Japan.

Conflict of interest

The authors who have taken part in this study declared that they do not have anything to disclose regarding funding or conflict of interest with respect to this manuscript.

Acknowledgments

We thank Ms. Masayo Baba and Ms. Nami Nishiyama for excellent technical assistance.

Supplementary data

Supplementary data associated with this article can be found, in the online version, at http://dx.doi.org/10.1016/j.jhep.2013.08.024.

References

[1] Nowell PC. The clonal evolution of tumor cell populations. Science 1976;194:23–28.
[2] Hanahan D, Weinberg RA. Hallmarks of cancer: the next generation. Cell 2011;144:646–674.
[3] Jordan CT, Guzman ML, Noble M. Cancer stem cells. N Engl J Med 2006;355:1253–1261.
[4] Clarke MF, Dick JE, Dirks PB, Eaves CJ, Jamieson CH, Jones DL, et al. Cancer stem cells–perspectives on current status and future directions: AACR Workshop on cancer stem cells. Cancer Res 2006;66:9339–9344.
[5] Dean M, Fojo T, Bates S. Tumour stem cells and drug resistance. Nat Rev Cancer 2005;5:275–284.
[6] Visvader JE, Lindeman GJ. Cancer stem cells in solid tumours: accumulating evidence and unresolved questions. Nat Rev Cancer 2008;8:755–768.
[7] Jemal A, Bray F, Center MM, Ferlay J, Ward E, Forman D. Global cancer statistics. CA Cancer J Clin 2011;61:69–90.
[8] Yamashita T, Forgues M, Wang W, Kim JW, Ye Q, Jia H, et al. EpCAM and alpha-fetoprotein expression defines novel prognostic subtypes of hepatocellular carcinoma. Cancer Res 2008;68:1451–1461.
[9] Yamashita T, Ji J, Budhu A, Forgues M, Yang W, Wang HY, et al. EpCAM-positive hepatocellular carcinoma cells are tumor-initiating cells with stem/progenitor cell features. Gastroenterology 2009;136:1012–1024.
[10] Yamashita T, Budhu A, Forgues M, Wang XW. Activation of hepatic stem cell marker EpCAM by Wnt-beta-catenin signaling in hepatocellular carcinoma. Cancer Res 2007;67:10831–10839.
[11] de Celis JF, Barrio R. Regulation and function of spalt proteins during animal development. Int J Dev Biol 2009;53:1385–1398.
[12] Aguila JR, Liao W, Yang J, Avila C, Hagag N, Senzel L, et al. SALL4 is a robust stimulator for the expansion of hematopoietic stem cells. Blood 2011;118:576–585.
[13] Yang J, Chai L, Gao C, Fowles TC, Alipio Z, Dang H, et al. SALL4 is a key regulator of survival and apoptosis in human leukemic cells. Blood 2008;112:805–813.
[14] Yang J, Chai L, Liu F, Fink LM, Lin P, Silberstein LE, et al. Bmi-1 is a target gene for SALL4 in hematopoietic and leukemic cells. Proc Natl Acad Sci U S A 2007;104:10494–10499.
[15] Yamashita T, Honda M, Nio K, Nakamoto Y, Takamura H, Tani T, et al. Oncostatin m renders epithelial cell adhesion molecule-positive liver cancer stem cells sensitive to 5-fluorouracil by inducing hepatocytic differentiation. Cancer Res 2010;70:4687–4697.
[16] Yamashita T, Honda M, Takatori H, Nishino R, Minato H, Takamura H, et al. Activation of lipogenic pathway correlates with cell proliferation and poor prognosis in hepatocellular carcinoma. J Hepatol 2009;50:100–110.
[17] Woo HG, Wang XW, Budhu A, Kim YH, Kwon SM, Tang ZY, et al. Association of TP53 mutations with stem cell-like gene expression and survival of patients with hepatocellular carcinoma. Gastroenterology 2011;140:1063–1070.
[18] Ji J, Wang XW. Clinical implications of cancer stem cell biology in hepatocellular carcinoma. Semin Oncol 2012;39:461–472.

[19] Yang J, Corsello TR, Ma Y. Stem cell gene SALL4 suppresses transcription through recruitment of DNA methyltransferases. J Biol Chem 2012;287: 1996–2005.
[20] Bohm J, Sustmann C, Wilhelm C, Kohlhase J. SALL4 is directly activated by TCF/LEF in the canonical Wnt signaling pathway. Biochem Biophys Res Commun 2006;348:898–907.
[21] Gao C, Dimitrov T, Yong KJ, Tatetsu H, Jeong HW, Luo HR, et al. Targeting transcription factor SALL4 in acute myeloid leukemia by interrupting its interaction with an epigenetic complex. Blood 2013;121:1413–1421.
[22] Lu J, Jeong HW, Kong N, Yang Y, Carroll J, Luo HR, et al. Stem cell factor SALL4 represses the transcriptions of PTEN and SALL1 through an epigenetic repressor complex. PLoS One 2009;4:e5577.
[23] Al-Baradie R, Yamada K, St Hilaire C, Chan WM, Andrews C, McIntosh N, et al. Duane radial ray syndrome (Okihiro syndrome) maps to 20q13 and results from mutations in SALL4, a new member of the SAL family. Am J Hum Genet 2002;71:1195–1199.
[24] Kohlhase J, Heinrich M, Schubert L, Liebers M, Kispert A, Laccone F, et al. Okihiro syndrome is caused by SALL4 mutations. Hum Mol Genet 2002;11:2979–2987.
[25] Rao S, Zhen S, Roumiantsev S, McDonald LT, Yuan GC, Orkin SH. Differential roles of Sall4 isoforms in embryonic stem cell pluripotency. Mol Cell Biol 2010;30:5364–5380.
[26] Tanimura N, Saito M, Ebisuya M, Nishida E, Ishikawa F. Stemness-related factor sall4 interacts with transcription factors oct-3/4 and sox2 and occupies oct-sox elements in mouse embryonic stem cells. J Biol Chem 2013;288:5027–5038.
[27] Wu Q, Chen X, Zhang J, Loh YH, Low TY, Zhang W, et al. Sall4 interacts with nanog and co-occupies nanog genomic sites in embryonic stem cells. J Biol Chem 2006;281:24090–24094.
[28] Yang J, Chai L, Fowles TC, Alipio Z, Xu D, Fink LM, et al. Genome-wide analysis reveals Sall4 to be a major regulator of pluripotency in murine-embryonic stem cells. Proc Natl Acad Sci U S A 2008;105:19756–19761.
[29] Yang J, Gao C, Chai L, Ma Y. A novel SALL4/OCT4 transcriptional feedback network for pluripotency of embryonic stem cells. PLoS One 2010;5:e10766.
[30] Zhang J, Tam WL, Tong GQ, Wu Q, Chan HY, Soh BS, et al. Sall4 modulates embryonic stem cell pluripotency and early embryonic development by the transcriptional regulation of Pou5f1. Nat Cell Biol 2006;8:1114–1123.
[31] Tsubooka N, Ichisaka T, Okita K, Takahashi K, Nakagawa M, Yamanaka S. Roles of Sall4 in the generation of pluripotent stem cells from blastocysts and fibroblasts. Genes Cells 2009;14:683–694.
[32] Yang J, Liao W, Ma Y. Role of SALL4 in hematopoiesis. Curr Opin Hematol 2012;19:287–291.
[33] Oikawa T, Kamiya A, Kakinuma S, Zeniya M, Nishinakamura R, Tajiri H, et al. Sall4 regulates cell fate decision in fetal hepatic stem/progenitor cells. Gastroenterology 2009;136:1000–1011.
[34] Ikeda H, Sato Y, Yoneda N, Harada K, Sasaki M, Kitamura S, et al. Alpha-Fetoprotein-producing gastric carcinoma and combined hepatocellular and cholangiocarcinoma show similar morphology but different histogenesis with respect to SALL4 expression. Hum Pathol 2012;43:1955–1963.
[35] Oikawa T, Kamiya A, Zeniya M, Chikada H, Hyuck AD, Yamazaki Y, et al. SALL4, a stem cell biomarker in liver cancers. Hepatology 2013;57:1469–1483.
[36] Gonzalez-Roibon N, Katz B, Chaux A, Sharma R, Munari E, Faraj SF, et al. Immunohistochemical expression of SALL4 in hepatocellular carcinoma, a potential pitfall in the differential diagnosis of yolk sac tumors. Hum Pathol 2013;44:1293–1299.
[37] Yong KJ, Gao C, Lim JS, Yan B, Yang H, Dimitrov T, et al. Oncofetal gene SALL4 in aggressive hepatocellular carcinoma. N Engl J Med 2013;368: 2266–2276.
[38] Lai AY, Wade PA. Cancer biology and NuRD: a multifaceted chromatin remodelling complex. Nat Rev Cancer 2011;11:588–596.
[39] Marquardt JU, Thorgeirsson SS. Sall4 in "stemness"-driven hepatocarcinogenesis. N Engl J Med 2013;368:2316–2318.

European Journal of Immunology

Adipose tissue derived stromal stem cell therapy in murine ConA-derived hepatitis is dependent on myeloid-lineage and CD4$^+$ T-cell suppression

Mami Higashimoto[*1], *Yoshio Sakai*[*2,3], *Masayuki Takamura*[1], *Soichiro Usui*[1], *Alessandro Nasti*[1], *Keiko Yoshida*[1], *Akihiro Seki*[1], *Takuya Komura*[1], *Masao Honda*[3], *Takashi Wada*[2], *Kengo Furuichi*[4], *Takahiro Ochiya*[5] *and Shuichi Kaneko*[1,3]

[1] Disease Control and Homeostasis, Kanazawa University, Kanazawa, Japan
[2] Department of Laboratory Medicine, Kanazawa University, Kanazawa, Japan
[3] Department of Gastroenterology, Kanazawa University Hospital, Kanazawa, Japan
[4] Division of Blood Purification, Kanazawa University Hospital, Kanazawa, Japan
[5] Division of Molecular and Cellular Medicine, National Cancer Center Research Institute, Tokyo, Japan

Mesenchymal stromal stem cells (MSCs) are an attractive therapeutic model for regenerative medicine due to their pluripotency. MSCs are used as a treatment for several inflammatory diseases, including hepatitis. However, the detailed immunopathological impact of MSC treatment on liver disease, particularly for adipose tissue derived stromal stem cells (ADSCs), has not been described. Here, we investigated the immunomodulatory effect of ADSCs on hepatitis using an acute ConA C57BL/6 murine hepatitis model. i.v. administration of ADSCs simultaneously or 3 h post injection prevented and treated ConA-induced hepatitis. Immunohistochemical analysis revealed higher numbers of CD11b$^+$, Gr-1$^+$, and F4/80$^+$ cells in the liver of ConA-induced hepatitis mice was ameliorated after the administration of ADSCs. Hepatic expression of genes affected by ADSC administration indicated tissue regeneration-related biological processes, affecting myeloid-lineage immune-mediating Gr-1$^+$ and CD11b$^+$ cells. Pathway analysis of the genes expressed in ADSC-treated hepatic inflammatory cells revealed the possible involvement of T cells and macrophages. TNF-α and IFN-γ expression was downregulated in hepatic CD4$^+$ T cells isolated from hepatitis livers co-cultured with ADSCs. Thus, the immunosuppressive effect of ADSCs in a C57BL/6 murine ConA hepatitis model was dependent primarily on the suppression of myeloid-lineage cells and, in part, of CD4$^+$ T cells.

Keywords: Adipose tissue derived stromal stem cells · Anti-inflammatory effects · CD4$^+$ T cells · ConA hepatitis · Myeloid-lineage cells

Additional supporting information may be found in the online version of this article at the publisher's web-site

Correspondence: Dr. Shuichi Kaneko
e-mail: skaneko@m-kanazwa.jp

*These authors contributed equally to this work.

Introduction

Mesenchymal stromal stem cells (MSCs) are somatic cells that reside in the mesenchymal tissues, such as the BM, umbilical cord, and adipose tissue [1,2]. MSCs are able to differentiate into several types of cells (pluripotent) in the same lineage, such as chondrocytes, osteocytes, adipocytes, and cardiomyocytes, as well as those of different lineages, such as hepatocytes. Because of this differentiation capability, they have been studied as a possible application in regenerative therapy of miscellaneous impaired organs, such as breast reconstruction [3] and repair of ischemic heart tissue [4]. Another intriguing characteristic of MSCs is their immunomodulatory potency [5]. Because most liver diseases, including viral hepatitis [6,7], primary biliary cirrhosis [8], autoimmune hepatitis [9], and steatohepatitis [10], are associated with hepatic inflammatory cells [11], elucidation of the effect of MSCs on hepatic inflammation is important when considering the use of MSCs for treating liver diseases. Although the efficacy of MSC treatment of liver diseases has been reported [12], the detailed immunopathological impact of MSC treatment on liver diseases, particularly for adipose tissue derived stromal stem cells (ADSCs), has not been investigated.

ConA, a plant lectin [13], is frequently used to induce acute hepatitis in rodents [14] to model the pathological features of autoimmune hepatitis. Although this model is mediated mainly by lymphocyte-lineage cells such as T cells and NKT cells, Kupffer cells/macrophages also participate in hepatitis. Therefore, evaluating the therapeutic efficacy of ADSCs in this murine hepatitis model is important. Although the potential efficacy of ADSCs in a BALB/c ConA hepatitis model has been reported [15], the immunopathology has not been investigated.

We confirmed that immediate i.v. administration of ADSCs after ConA injection prevented hepatitis. We also observed that administering ADSCs 3 h after the ConA injection resulted in successful treatment of hepatitis, as the liver was already infiltrated by $CD11b^+$ and $Gr\text{-}1^+$ inflammatory cells. Gene expression analysis of the liver showed that ADSC treatment affected myeloid-lineage cells, providing repair and regenerative effects in ConA-induced hepatitis mice. Moreover, gene expression analysis of hepatic inflammatory cells indicated pathways related to T cells and monocyte-lineage cells. Pathologically important cytokines such as TNF-α and IFN-γ were upregulated in $CD4^+$ T cells isolated from ConA-induced hepatitis mice but were significantly suppressed by co-culture with ADSCs. Thus, the anti-inflammatory effects of ADSCs in the C57BL/6 murine ConA hepatitis model were mediated by the suppression of myeloid-lineage and $CD4^+$ T cells.

Results

Characteristics of the immune response in ConA-induced hepatitis mice

To examine the characteristics of ConA-induced acute hepatitis, we injected 300 μg ConA into C57BL/6 female mice ($n = 4$) and determined serum alanine transferase (ALT) and lactate dehydrogenase (LDH) activities. Serum ALT and LDH activities were elevated through 24 h (Fig. 1A). The macroscopic appearance and histology of the liver obtained 24 h after ConA injection revealed intense necrosis (Fig. 1B). The immunohistochemical analysis showed that the number of $CD4^+$ T cells in the liver peaked at 6 h after the ConA injection, and remained high for 24 h (Fig. 1C and D). The numbers of $CD11b^+$ cells and $Gr\text{-}1^+$ cells accumulated in the liver increased at 3 h and reached a maximum at 12 h after ConA injection (Fig. 1C and D). The numbers of $F4/80^+$ monocyte/macrophage lineage cells increased at 6 h after the ConA injection, but returned to basal levels after 24 h (Fig. 1C and D). We also assessed the frequency of $CD11b^+/Gr\text{-}1^+$ cells, as a phenotype of myeloid-derived suppressor cells (MDSCs), in ConA hepatitis mice at 6 h ($n = 3$). The frequency of $CD11b^+/Gr\text{-}1^+$ cells was higher than that in WT mice (Fig. 1E). Scavenger receptor CD204 expression was higher in $CD11b^+/Gr\text{-}1^+$ cells than $CD11b^+/Gr\text{-}1^-$ cells (Fig. 1F), and the population gated for $CD11b^+$ cells contained granulocytic $Ly\text{-}6C^+/Ly\text{-}6G^+$ cells as well as monocytic $Ly\text{-}6C^+/Ly\text{-}6G^-$ cells (Fig. 1G).

To determine the type of immune-mediating cells involved in ConA-induced acute hepatitis, we depleted mice of various immune cell subpopulations ($n = 4$ per group). Mice that were pretreated with clodronate, a reagent that depletes monocyte-macrophage lineage cells [16], followed by injection of ConA, did not show a significant elevation in serum ALT or LDH activity (Fig. 1H). Mild elevation of serum activity for these enzymes in mice depleted of $CD4^+$ T cells was observed, whereas depletion of $CD8^+$ T cells had no significant effect. These results suggest the importance of monocyte-macrophage myeloid-lineage cells, as well as the contribution of $CD4^+$ T cells, in ConA-induced hepatitis.

ConA-induced acute hepatitis is ameliorated by i.v. administration of ADSCs in vivo

Next, we determined the therapeutic efficacy of ADSCs in the ConA-induced hepatitis model. We obtained and expanded stromal cells from adipose tissue by passaging them eight to ten times (Fig. 2A). Almost all cells expressed the mesenchymal lineage markers, CD29 and CD44 (Fig. 2B). With regard to stem cell markers [17], approximately 40% and 73% of cells expressed CD105 and CD90, respectively (Fig. 2B). Moreover, the cells were pluripotent and were able to differentiate into osteocytes, chondrocytes, and adipocytes (Fig. 2C–F). When 1×10^5 ADSCs were administered via the tail vein immediately after ConA injection in mice ($n = 3$), the elevation of serum ALT and LDH activity was substantially ameliorated, compared with mice without ADSC treatment ($n = 4$) 24 h after injection (Fig. 3A). In terms of therapeutic efficacy, 1×10^5 ADSCs were administered to mice 3 h after ConA injection ($n = 3$), serum ALT and LDH activities were significantly reduced in acute hepatitis mice treated with ADSCs, compared with ConA-induced hepatitis mice without treatment ($n = 4$), 24 h after ConA administration (Fig. 3B). The macroscopic

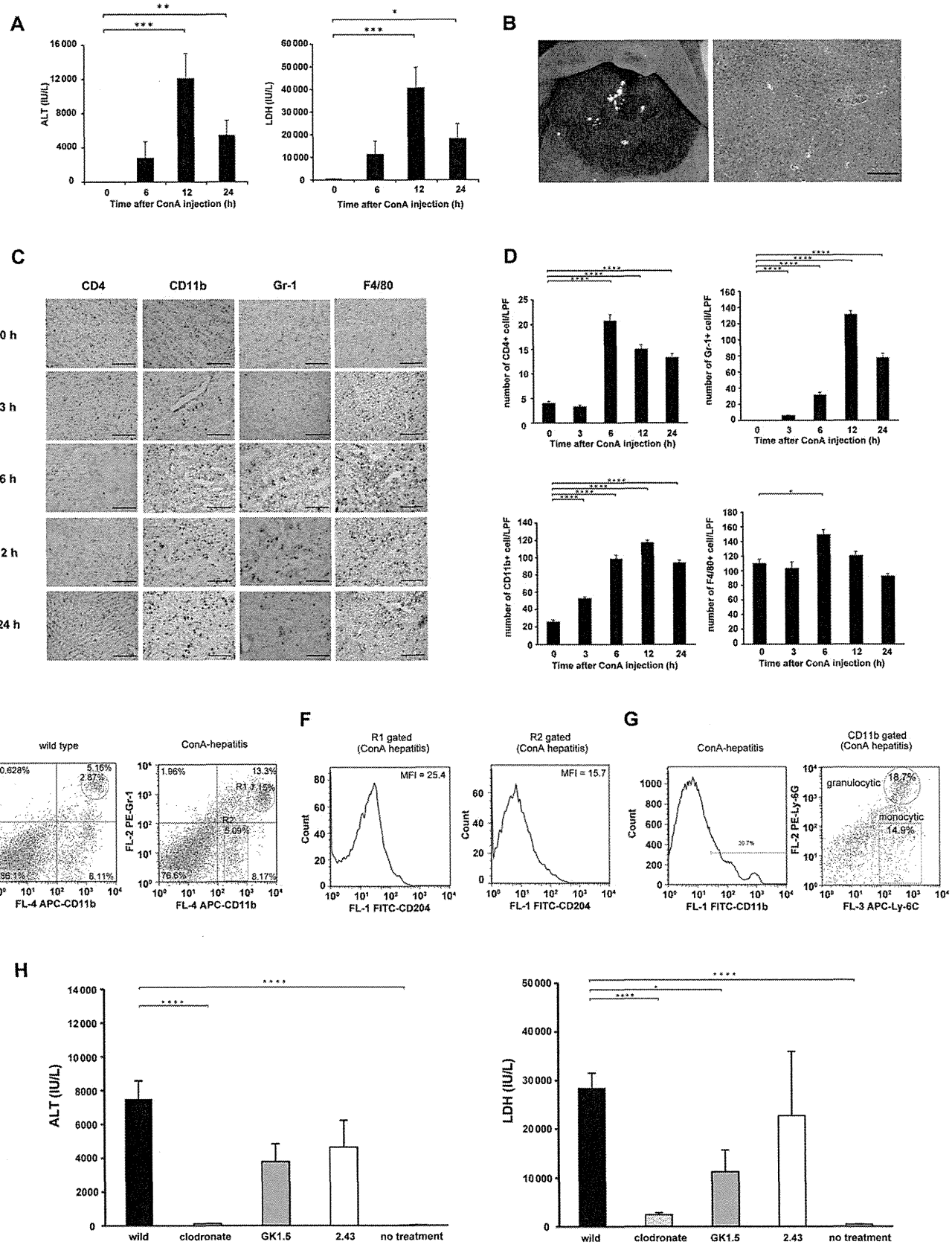

appearance of the liver obtained from mice injected with 300 μg of ConA followed by ADSC administration showed a mild and spotty white area with an almost normal color (Fig. 3C). Liver histology showed an almost normal appearance, with no necrosis (Fig. 3C), indicating that ConA-induced hepatitis was markedly ameliorated by ADSC treatment. No preventive or therapeutic effect on ConA-induced hepatitis resulted from administration of primary cultured murine hepatocytes ($n = 3$); there was no significant reduction in serum ALT or LDH (Fig. 3A and B), macroscopic necrosis appearance, or histological necrosis, compared with ConA-induced hepatitis (Fig. 3C).

ADSC treatment reduces elevated cytokine/chemokine concentrations in ConA-induced hepatitis mice

Marked protective and therapeutic effects of ADSCs on ConA-induced hepatitis were observed. To determine the effect of ADSC treatment on systemic inflammation in ConA-induced hepatitis, we measured serum cytokine and chemokine concentrations in ConA-induced hepatitis mice treated with ADSCs. Mice injected with ConA were immediately treated with ADSCs and serum was collected 6 h after ConA injection ($n = 3$). The elevated serum IFN-γ, IL-2, IL-6, IL-4, IP-10, MIG, KC, and MCP-1 levels in ConA-injected mice ($n = 3$) were significantly reduced by ADSC treatment (Supporting Information Fig. 1A). Injection of mice with ADSCs 3 h after ConA administration ($n = 4$) resulted in significantly reduced serum IFN-γ, IL-2, IL-6, and MIG levels, compared to ConA-injected mice not treated with ADSCs ($n = 6$) (Supporting Information Fig. 1B). Thus, the levels of the array of cytokines and chemokines that are elevated in the sera of ConA-induced hepatitis mice were significantly decreased by ADSC treatment.

Distribution of i.v. administered ADSCs in ConA-induced hepatitis murine models

The distribution of administered ADSCs in ConA-induced hepatitis mice was determined by immunohistochemistry. Administered GFP-expressing ADSCs were observed in the lung, but not the liver, of mice injected with ConA followed by immediate ADSC administration ($n = 6$), through 24 h (Supporting Information Fig. 2A). When administered to mice 3 h after ConA injection ($n = 6$), GFP-expressing ADSCs were observed primarily in the lung, and a few in the liver (Supporting Information Fig. 2B), suggesting that some fraction of ADSCs reached the liver upon occurrence of hepatitis.

Hepatic gene expression changes by ADSCs treatment are associated with Gr-1$^+$ and CD11b$^+$ cells

To investigate the detailed biological features of the liver in ConA-induced hepatitis mice that were treated with ADSCs, we examined the gene expression profiles of liver tissue of ConA-injected mice obtained 2 h after treatment with ADSCs using a DNA microarray. In the liver tissues of mice treated with ADSCs immediately after ConA injection ($n = 3$), 589 gene probes were differentially expressed compared with that in mice with ConA-induced hepatitis that had not been treated with ADSCs ($n = 3$). Expression of the majority of genes was downregulated by ADSCs, as shown by green color ($p < 0.05$; Fig. 4A). Principal component analysis using these genes showed a discernible distribution difference between the ADSC-treated and -untreated groups (Fig. 4B). When mice received ADSC treatment 3 h after ConA injection, hepatic expression of 309 gene probes was altered significantly compared with those in mice with ConA-induced hepatitis that had not been treated with ADSCs ($n = 3$). Expression of the majority of genes was downregulated by ADSCs, as shown by green color ($p < 0.01$; Fig. 4C). Principal component analysis of these genes also showed a discernible distribution difference between the ADSC-treated and untreated groups (Fig. 4D). In the context of biological maps of the genes affected by immediate ADSC treatment, cell differentiation, the inflammatory response, the DNA damage response, and apoptosis predominated (Supporting Information Table 1). In addition to these maps, tissue remodeling and wound repair, mitogenic signaling, and vascular development (angiogenesis) predominated in mice that had received ADSC treatment 3 h after ConA injection (Table 1), indicating that ADSCs provided not only anti-inflammatory effects, but also remodeling effects, in the ConA-damaged liver.

◀ **Figure 1.** Characteristics of ConA-induced hepatitis in C57BL/6 mice. (A–D) C57BL/6 female mice were injected i.v. with 300 μg of ConA. Sera and liver tissues were obtained 3, 6, 12, and 24 h after ConA injection. The data are representative of three individual experiments. (A) ALT and LDH activity in sera. Results are expressed as means ± SE ($n = 4$). $^*p < 0.05$, $^{**}p < 0.01$, $^{***}p < 0.005$ versus 0 h (Student's t-test). (B) Representative liver tissues obtained 12 h after ConA injection were assessed macroscopically and microscopically. Magnification: ×100. Bar: 200 μm. (C) Immunohistochemical staining for CD4, CD11b, Gr-1, and F4/80 in the livers of mice for each time point (0, 3, 6, 12, and 24 h; $n = 4$ per time point). Representative images of mice for each time point are shown. Magnification: ×100. Bar: 200 μm. (D) Quantification of the number of CD4$^+$, CD11b$^+$, Gr-1$^+$, and F4/80$^+$ cells in four visual fields per ×100 low-power field in the livers of representative mice in each group. Magnification: ×100. $^*p < 0.05$, $^{****}p < 0.001$ versus untreated mice (Student's t-test). (E–G) Hepatic inflammatory cells were isolated from mice 6 h after ConA injection, incubated with fluorescence-conjugated antibodies, and assessed by FACS. Three mice per group per experiment. Experiments were performed twice. (E) Frequency of CD11b$^+$Gr-1$^+$ cells in WT C57BL/6 mice and ConA hepatitis mice. (F) Analysis of CD204 expression in CD11b$^+$Gr-1$^+$ cells (R1-gated region in (E)) and CD11b$^+$Gr-1$^-$ cells (R2-gated region in (E)) among hepatic inflammatory cells from ConA hepatitis mice. MFI: mean fluorescence intensity. (G) CD11b$^+$ cells among hepatic inflammatory cells from ConA hepatitis mouse were gated, and Ly-6C and Ly-6G expression levels in the gated cells were determined. (H) C57BL/6 female mice were injected i.v. with clodronate ($n = 4$), i.p. with anti-CD4 antibody (GK1.5) ($n = 4$), or anti-CD8 antibody (2.43) ($n = 4$) every 24 h for 2 days. The mice were then injected i.v. with 300 μg of ConA. Sera were obtained 24 h after ConA injection, and ALT and LDH activities were then measured. Results are expressed as means +SE ($n = 4$ per group) and are representative of one experiment performed. $^*p < 0.05$, $^{****}p < 0.001$ versus ConA-injected WT mice ($n = 4$) (Student's t-test).

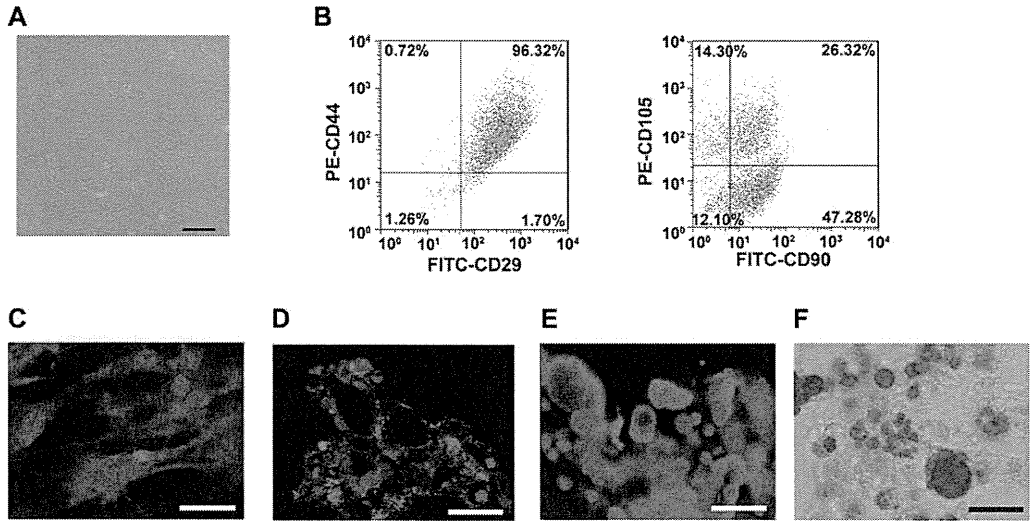

Figure 2. Characteristics and pluripotency of cultured ADSCs. Cells in the stromal fraction of adipose tissues from mice were cultured, maintained, and expanded for eight to ten passages. (A) Spindle shaped cells were observed after eight passages. Magnification: ×100. Bar: 200 μm. (B) Flow cytometric analysis of CD29, CD44, CD90, and CD105 surface marker expression. The data shown are representative of three independent experiments. (C–F) ADSCs were cultured with specific growth factors for induction of osteocytes, chondrocytes, and adipocytes using a mouse mesenchymal stem cell functional kit. Immunohistochemical staining was performed with (C) anti-osteopontin antibody for osteocytes, (D) anti-collagen II antibody for chondrocytes, and (E) anti-FABP antibody as well as (F) Oil-Red O staining for adipocytes. Magnification: x200. Bars: 50 μm. All data shown are from one experiment representative of two independent experiments performed.

Next, we investigated the relevance of these altered genes in the context of inflammatory cells using the public gene expression database of hematopoietic cells and stem cells (GSE27787). The annotated genes among the 589 gene probes detected by microarray analysis probes in the livers of mice that received ADSC treatment immediately after ConA injection were not relevant to any hematopoietic cell type (Fig. 4E). By contrast, among the 309 gene probes, the majority of the annotated genes whose hepatic expression in mice that received ADSC treatment 3 h after ConA injection was affected significantly were found to be highly expressed in Gr-1$^+$ cells and Mac1$^+$ (CD11b$^+$) cells — as indicated by the red color (Fig. 4F). Since majority of the 309 gene probes in the liver of ConA hepatitis were downregulated by ADSC treatment, as indicated by green color (Fig. 4C), these results suggested that effects on Gr-1$^+$ and CD11b$^+$ cells were associated with the therapeutic effect of ADSCs 3 h after ConA injection.

ADSC treatment represses inflammatory cell accumulation in ConA-induced hepatitis

To determine the influence of ADSC treatment on the infiltration/accumulation of immune-mediating cells in the liver of ConA-induced hepatitis mice, we assessed by immunohistochemistry the inflammatory cells in the liver tissues of mice injected with ConA followed by ADSC administration at 3 h. Liver tissues obtained at 6, 12, and 24 h (n = 4 each time point) after ConA injection showed reduced accumulation of CD11b$^+$ cells, Gr-1$^+$ cells, and F4/80$^+$ cells after ADSC treatment (Fig. 5). In contrast, the increased number of infiltrated CD4$^+$ T cells in ConA-induced hepatitis mice was not significantly affected by the ADSCs (Fig. 5). Thus, the predominant change in ConA-induced hepatitis mice treated with ADSCs was in the number of myeloid-lineage inflammatory cells, consistent with the hepatic gene expression data.

T-cell involvement in the altered gene expression of hepatic inflammatory cells by ADSCs treatment

To further assess the anti-inflammatory effects of ADSCs in mice with ConA-induced hepatitis, we isolated hepatic inflammatory cells from mice 2 h after ADSC treatment, which was administered 3 h after ConA injection (n = 2) and from mice not treated with ADSCs (n = 2). A total of 939 genes were differentially expressed in hepatic inflammatory cells from ConA-induced hepatitis mice treated with ADSCs. The gene expression profiles associated with ADSC treatment and ConA-induced hepatitis without ADSC treatment were readily distinguishable (Supporting Information Fig. 3A). Pathway map analysis showed that these genes were relevant to biological pathways of oncostatin M signaling via JAK-Stat or MAPK signaling and CCR5 signaling in macrophages and T lymphocytes in the immune response pathway (Supporting Information Table 2). Network analysis of these genes featured a network consisting of AcRIIA, STAT3, Activin A, FTSJD1, and STAT1 at the top (Supporting Information Table 3), which indicated that pathways involving IL-2 and TNF-α, and the STAT1/STAT3 pathway were also involved (Supporting Information Fig. 3B). These results suggest that T cells, as well as antigen presenting/phagocytosis lineages, were the immune-mediating cell populations affected by ADSC treatment.

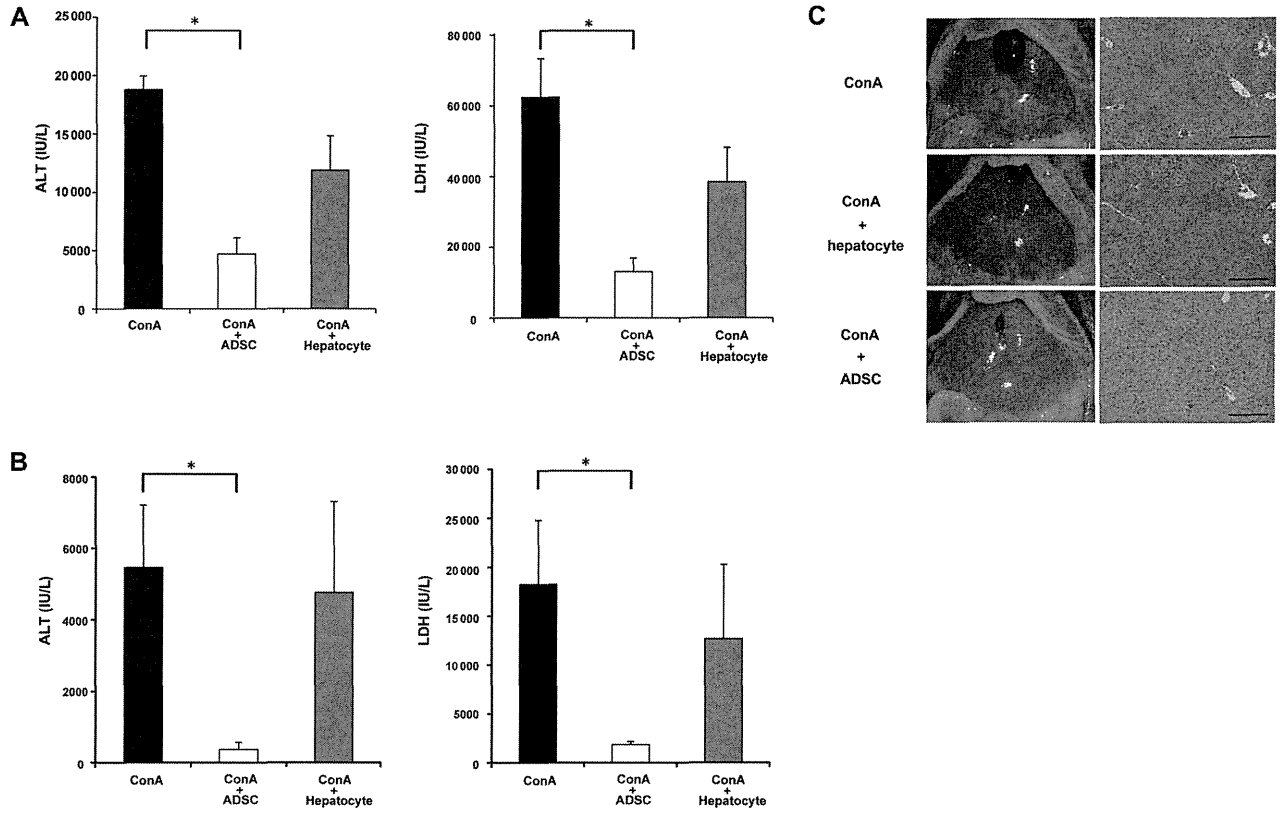

Figure 3. Therapeutic effects of ADSCs in ConA-induced hepatitis. C57BL/6 female mice were injected i.v. with 300 μg of ConA. Immediately or 3 h later, 1×10^5 ADSCs or hepatocytes were injected via the tail vein. Liver tissues and blood samples were obtained 24 h after ConA injection. Liver tissues were examined histologically and serum ALT and LDH activities were measured. (A, B) Serum ALT and LDH activities of mice injected with ConA followed by ADSC injection (A) immediately or (B) 3 h later. ConA: ConA-injected mice without treatment ($n = 4$), ConA + ADSC: ConA-injected mice followed by ADSC treatment ($n = 3$), ConA + hepatocyte: ConA-injected mice followed by primary cultured hepatocyte treatment ($n = 3$). Data are shown as mean ± SE and are from one experiment representative of two independent experiments. $^*p < 0.05$ (Wilcoxon signed-rank test), compared with ConA-injected mice. (C) Macroscopic appearance of the liver (left) and histology of the liver tissues as assessed by H&E staining (right). Magnification of histology: ×100. Bars: 200 μm. Images shown are from one mouse representative of three to four mice from each group studied.

ConA-activated CD4$^+$T cells and CD11b$^+$ cells in the liver are important targets of ADSC treatment

The above data indicated that ADSCs administered in ConA-induced hepatitis had therapeutic immunological effects in terms of repairing the damaged liver and affected CD11b$^+$ and Gr-1$^+$ myeloid-lineage cells and T cells. To further explore how ADSCs affected the subpopulations of inflammatory cells involved in ConA-induced hepatitis, we investigated the expression of cytokine/chemokine-related genes in CD4$^+$ T cells and CD11b$^+$ cells obtained from livers with ConA-induced hepatitis ($n = 4$) that had been treated in vitro with ADSCs ($n = 3$). Expression of TNF-α, IL-10, and CXCL10 was significantly downregulated by ADSC treatment in both CD4$^+$ T cells (Supporting Information Fig. 4A) and CD11b$^+$ cells (Supporting Information Fig. 4B). IFN-γ, IL-4, and CXCL9 expression by CD4$^+$ T cells were significantly affected by ADSCs. Although CCL3, which was upregulated by ConA injection, was not significantly affected by ADSCs, the expression of its cognate receptor, CCR5, was decreased in CD4$^+$ T cells (Supporting Information Fig. 4A), suggesting an effect on the CCL3-CCR5 axis. These results suggest that CD4$^+$ T cells and myeloid-lineage CD11b$^+$ cells were the susceptible hepatic inflammatory subpopulations of cells in the ConA-induced hepatitis liver.

Anti-inflammatory effect of ADSCs on ConA hepatitis do not rely on MDSCs

We further assessed whether the anti-inflammatory effect of ADSCs in ConA hepatitis relied on MDSCs. Neither the frequency of nor the NO production by CD11b$^+$Gr-1$^+$ cells were increased by ADSC treatment (Supporting Information Fig. 5A). CD11b$^+$Gr-1$^+$ cells from ConA-injected mice treated with ADSCs showed arginase activity similar to that in CD11b$^+$Gr-1$^+$ cells from ConA-injected mice (Supporting Information Fig. 5B). CD11b$^+$Gr-1$^+$ cells from ConA-injected mice treated with ADSCs suppressed the ConA-stimulated proliferation of T cells in vitro, although the effect was slightly attenuated compared to that of cells from mice with ConA-induced hepatitis (Supporting Information Fig. 5C). Thus, ADSC treatment was not dependent on MDSCs induced by ConA hepatitis.

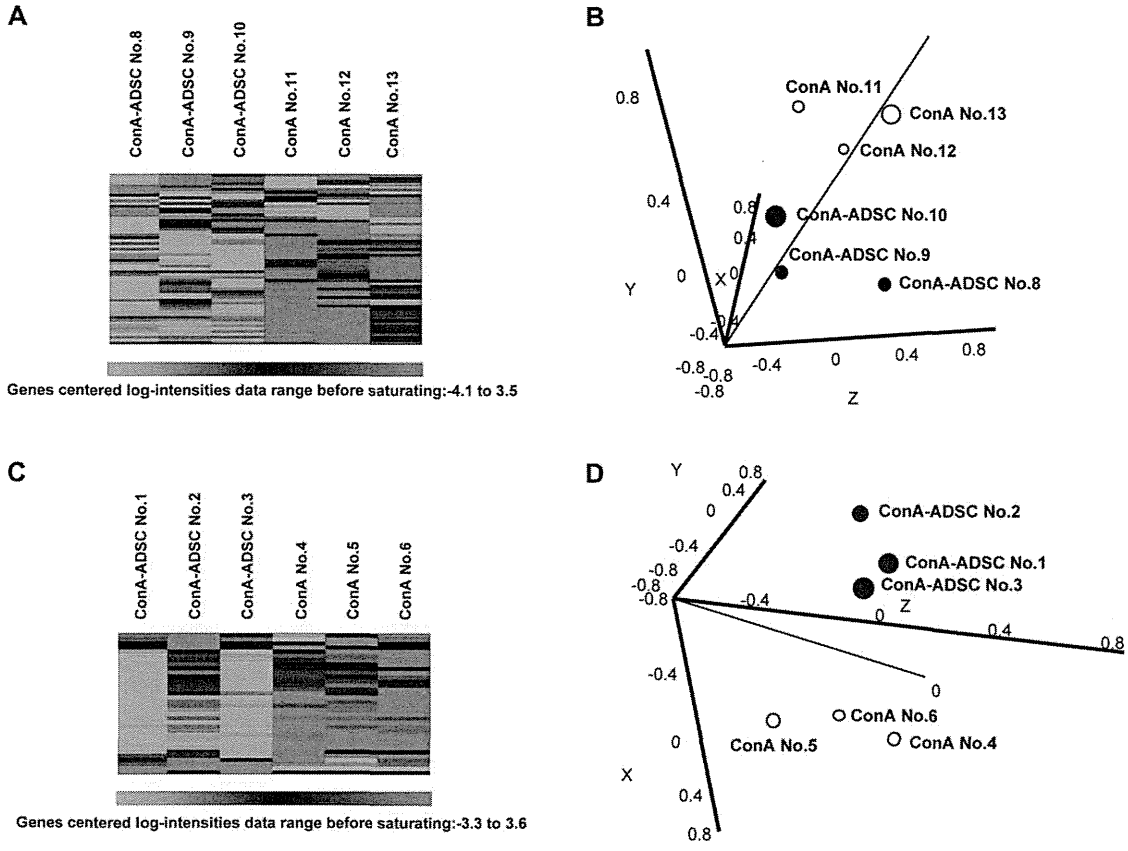

Discussion

MSCs are effective for immune-mediated disease treatment including the ConA-induced BALB/c murine hepatitis model [15], but the detailed mechanisms have not been fully elucidated. Here, we confirmed that ADSCs have preventive and therapeutic effects in a ConA-induced C57BL/6 hepatitis murine model and assessed the immunopathological mechanisms by determining the participating hepatic immunomodulatory cells. ADSCs injected via the tail vein were found in the lung; some were observed in the liver but only when ADSCs were administered 3 h after ConA injection, a time at which infiltration of $CD11b^+$ and $Gr\text{-}1^+$ inflammatory cells into the liver had already begun. Gene expression analysis of liver tissue from ConA-induced hepatitis mice showed that the ADSC treatment induced biological pathways indicative of liver repair and regeneration. Myeloid-lineage cells were the predominant population in terms of affected genes, consistent with immunohistochemical staining of the liver for immune-mediating cells. Furthermore, the gene expression profiles of hepatic inflammatory cells from ConA-induced hepatitis mice treated with ADSCs suggested T-cell and macrophage involvement. Moreover, the expression patterns of cytokine/chemokine-related genes in hepatic inflammatory cells co-cultured with ADSCs suggested that $CD4^+$ T cells were important in ConA-induced hepatitis and were affected by ADSC treatment.

The immunopathological features of ConA-induced hepatitis have been characterized as being primarily lymphocyte-lineage cell-mediated hepatitis [18–20], leading to massive hepatocellular degeneration, necrosis, and apoptosis [21]; thus, this model is relevant to clinical autoimmune hepatitis. Additionally, Kupffer cells play an important role in induction of hepatitis [22]. Unexpectedly, we observed prominent increases in $CD11b^+$, $Gr\text{-}1^+$, and $F4/80^+$ cells in liver tissues of the ConA-induced hepatitis mice. Additionally, we found that the monocyte-macrophage lineage cells contributed most significantly to hepatitis, as confirmed by depletion treatment, such that hepatitis was almost completely abolished when those cell types were abrogated by clodronate. This is further evidenced by the fact that ADSC treatment reduced the number of $CD11b^+$, $Gr\text{-}1^+$, and $F4/80^+$ cells in the liver of ConA-induced hepatitis mice (Fig. 5). The importance of $Gr\text{-}1^+$ and $CD11b^+$ cells was also suggested by changes in the gene expression profile of the liver of ConA-induced hepatitis treated with ADSCs (Fig. 4C and F). Thus, monocyte-macrophage lineage cells are important in the pathogenesis of ConA-induced hepatitis in mice and are important targets of ADSCs. $CD4^+$ T cells were also involved since their depletion partially ameliorated ConA-induced hepatitis. The number of infiltrating $CD4^+$ T cells in the liver of ConA-induced hepatitis mice was not markedly reduced by ADSC treatment. However, gene expression analysis of hepatic inflammatory cells in ConA-induced hepatitis mice treated with ADSCs showed that signaling of oncostatin M, a type I cytokine associated with developing T cells [23], and CCR5 signaling in macrophages and T lymphocytes were affected. Therefore, $CD4^+$ T cells participate as an immune mediator and therapeutic target of ADSCs in the pathology of ConA-induced hepatitis mice.

With regard to cytokine/chemokine-related gene expression in hepatic inflammatory cells of ConA-induced hepatitis mice, expression of TNF-α, IL-10, and CXCL10 in $CD4^+$ T cells and $CD11b^+$ cells was downregulated by ADSC treatment (Supporting Information Fig. 4). Additionally, IFN-γ, IL-4, and CXCL9 were also significantly downregulated in $CD4^+$ T cells, but not in $CD11b^+$ cells (Supporting Information Fig. 4). Changes in the expression of the Th2 cytokines, IL-10 and IL-4, were considered to be the secondary consequence of ConA-induced hepatitis, mediated by TNF-α and/or IFN-γ, which are characterized as Th1-associated cytokines [24]. CCR5 expression by $CD4^+$ T cells was downregulated by ADSCs, which may be relevant to the biological processes indicated by the downregulated genes in hepatic inflammatory cells. Because CCR5 is a $CD4^+$ T-cell receptor that interacts with APCs, such as macrophages [25], suppression of CCR5 expression on $CD4^+$ T cells by ADSC might explain the amelioration of ConA-mediated hepatitis. Overall, the therapeutic efficacy of ADSCs impacted both $CD4^+$ and $CD11b^+$ cells in terms of alteration of levels of inflammatory humoral mediators and cytokine/chemokine profiles, thus contributing to amelioration of ConA-induced hepatitis.

A proportion of i.v. administered ADSCs were present in the livers of ConA mice injected with ADSCs at a time point at which the liver had already been infiltrated with $Gr\text{-}1^+$ and $CD11b^+$ cells, whereas no ADSCs were present in the livers of mice injected with ConA following immediate treatment with ADSCs. This indicates that a liver undergoing inflammation attracts administered ADSCs. The extent of inflammation required to recruit ADSCs should be clarified, as it has previously been reported that hepatitis occurring just 30 min after ConA injection results in recruitment of a substantial number of stem cells to the liver in the BALB/c ConA hepatitis model [15]. Given that the migratory capabilities of MSCs are well known although not yet fully investigated [26], how ADSCs are recruited to an already inflamed liver as a result of ConA administration should be examined. In addition, the ADSCs administered to C57BL/6 mice immediately after ConA injection resided in the lung. In spite of the fact that they were not detected in the liver, these ADSCs prevented ConA hepatitis, indicating the remote effect of ADSCs. Thus, indirect mediators produced by ADSCs associated with their anti-inflammatory effects should be investigated intensively.

◀ **Figure 4.** Gene expression analysis in the liver of ConA-induced hepatitis mice treated with ADSCs. C57BL/6 female mice were injected i.v. with 300 μg of ConA. (A, B, and E) Immediately or (C, D, and F) 3 h after ConA injection, mice were treated with 1×10^5 ADSCs via the tail vein ($n = 3$ each). Liver tissues were analyzed 2 h after ADSC administration and RNA was isolated for gene expression analysis using a DNA microarray. Data shown are from one experiment performed. (A, B) One-way clustering analysis (A) and principal component analysis (B) of the 589 differentially expressed genes in treated and untreated ConA-injected mice. (C, D) One-way clustering analysis (C) and principal component analysis (D) of the 309 differentially expressed genes in treated (after 3 h) and untreated ConA-injected mice followed. Colors indicate the intensity of gene upregulation (red), downregulation (green), and no change (black). (E, F) One-way clustering analysis of gene expression in hematopoietic and stem cells (GSE27787) for annotated genes among the 589 (E) and 309 (F) genes.

Table 1. Maps relevant to genes for which the expression was affected in the liver of ConA-injected mice followed by ADSC treatment at 3 h.

Maps	*p*-value
Tissue remodeling and wound repair	0.000001438
Inflammatory response	0.000003973
Mitogenic signaling	0.0001056
Vascular development (angiogenesis)	0.0002926
DNA damage response	0.0004529
Apoptosis	0.0008909
Cystic fibrosis disease	0.001402
Myogenesis regulation	0.001571
Cell differentiation	0.002173
Immune system response	0.003304

In conclusion, the therapeutic anti-inflammatory efficacy of ADSCs relied on suppression of myeloid-lineage and $CD4^+$ T cells in the ConA-induced C57BL/6 murine hepatitis model. The application of ADSC therapy to various inflammatory liver diseases can be further developed by studies of their immunomodulatory effects.

Materials and methods

Murine acute hepatitis induced by ConA injection and treatment with ADSCs

C57BL/6J female mice (10–12 weeks old, Charles River Laboratories Japan Inc., Yokohama, Japan) were injected i.v. with 300 μg of ConA (Sigma-Aldrich, St. Louis, MO, USA) dissolved in PBS. For $CD4^+$ T-cell or $CD8^+$ T-cell depletion, 200 μg of purified anti-CD4 antibody from the culture supernatant of GK1.5 cells (ATCC, Manassas, VA, USA), or purified anti-CD8 antibody from the culture supernatant of 2.43 cells (ATCC), was injected i.p. for two consecutive days before ConA injection. For depletion of monocyte-macrophage lineage cells, 2 mg of clodronate (Sigma-Aldrich), which was encapsulated in liposomes using the COATSOME-EL-01-N liposome formulation kit (Nihonyushi, Tokyo, Japan) [27], was injected via the tail vein 2 days before ConA injection. For the prevention or treatment experiment, 1×10^5 ADSCs were administered i.v. immediately or 3 h after ConA injection. In some cohorts, blood was obtained under anesthesia, and liver and lung tissues were collected after euthanizing mice at 6, 12, and 24 h after ConA injection. A portion of the liver tissue was homogenized and the enriched fraction of inflammatory cells was obtained by gradient centrifugation using Ficoll–Hypaque (Sigma-Aldrich). Our institutional review board approved the care and use of laboratory animals in all experiments.

Isolation and culture of ADSCs and primary hepatocytes

Inguinal adipose tissues were obtained from C57BL/6J male mice (10–12 weeks old, Charles River Laboratories Japan Inc.) or GFP-transgenic mice (male, 10–12 weeks old, gift from Prof. Okabe, Osaka University, Japan). Tissues were digested with 0.075% collagenase type I (Wako Pure Chemical Industries Ltd., Osaka, Japan), washed with PBS, and then transferred to a culture dish with DMEM/F-12 1:1 medium (Life Technologies–Invitrogen, Carlsbad, CA, USA) supplemented with 10% heat-inactivated FBS and 1% antibiotic–antimycotic solution (Life Technologies). Cells were maintained and expanded by eight to ten passages before use.

To obtain primary hepatocytes, C57BL/6J male mice (10–12 weeks old) were anesthetized by i.p. injection of pentobarbital (50 mg/kg; Kyoritsu Seiyaku, Tokyo, Japan) and injected with 10 mL of 0.75% type I collagenase solution via the portal vein. Liver tissues were minced to dissociate cells, filtered through a 100 μm mesh, and cultured in 10-cm culture dishes for 16 h until use.

Pluripotency of ADSCs

The pluripotency of ADSCs was examined using a mouse mesenchymal stem cell functional kit® (R&D Systems, Minneapolis, MN, USA), and immunohistochemical staining of cells that had differentiated into osteocytes, chondrocytes, and adipocytes was performed using anti-mouse ostepontin, anti-mouse collagen II, and anti-mouse FABP4 antibodies, respectively, in accordance with the manufacturer's instruction. Adipocyte differentiation was also assessed by staining using an aliquot of Oil Red O (WAKO).

Co-culture of ConA-stimulated hepatic inflammatory cells with ADSCs

Hepatic inflammatory cells were isolated from C57BL/6J female mice (10 weeks old) that had been injected i.v. with 300 μg of ConA 3 h before ($n = 4$). $CD4^+$ T cells and $CD11b^+$ cells were separated from the collected hepatic inflammatory cells using anti-CD4 and anti-CD11b magnetic beads (Miltenyi Biotec, Bergisch Gladbach, Germany). Then, 20 000 ADSCs were co-cultured with 4×10^5 of the isolated $CD4^+$ T cells or $CD11b^+$ cells in a 24-well plate (BD Falcon, San Jose, CA, USA) for 2 h ($n = 3$). After co-culture, floating cells were harvested, and RNA harvested using the MicroRNA isolation kit (Stratagene, La Jolla, CA, USA) for real-time PCR analysis to measure cytokine/chemokine gene expression.

Measurement of serum ALT and LDH activity

Blood was collected from the postorbital venous plexus and serum was separated from clotted blood after coagulation. The serum activity of ALT, and LDH was measured using L-type WAKO GPT J2, and LDH-J kits (Wako Pure Chemical Industries Ltd.), respectively, using autoanalytical equipment (Hitach7180, Hitachi Ltd., Tokyo, Japan), according to the manufacturer's protocol.

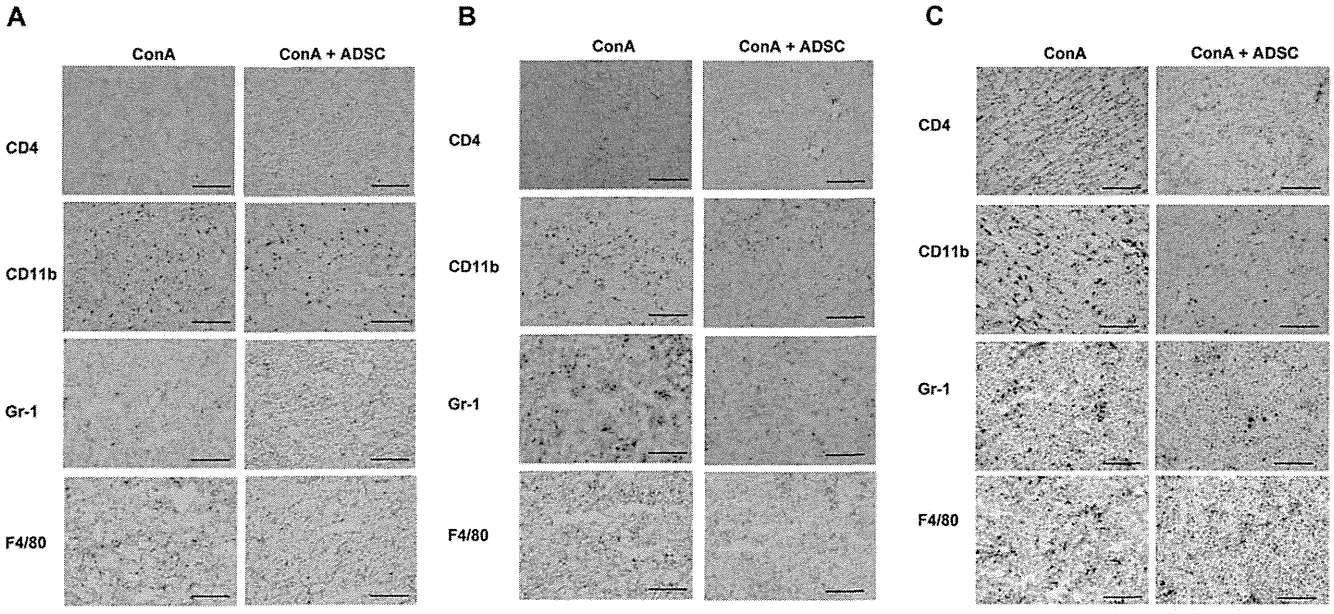

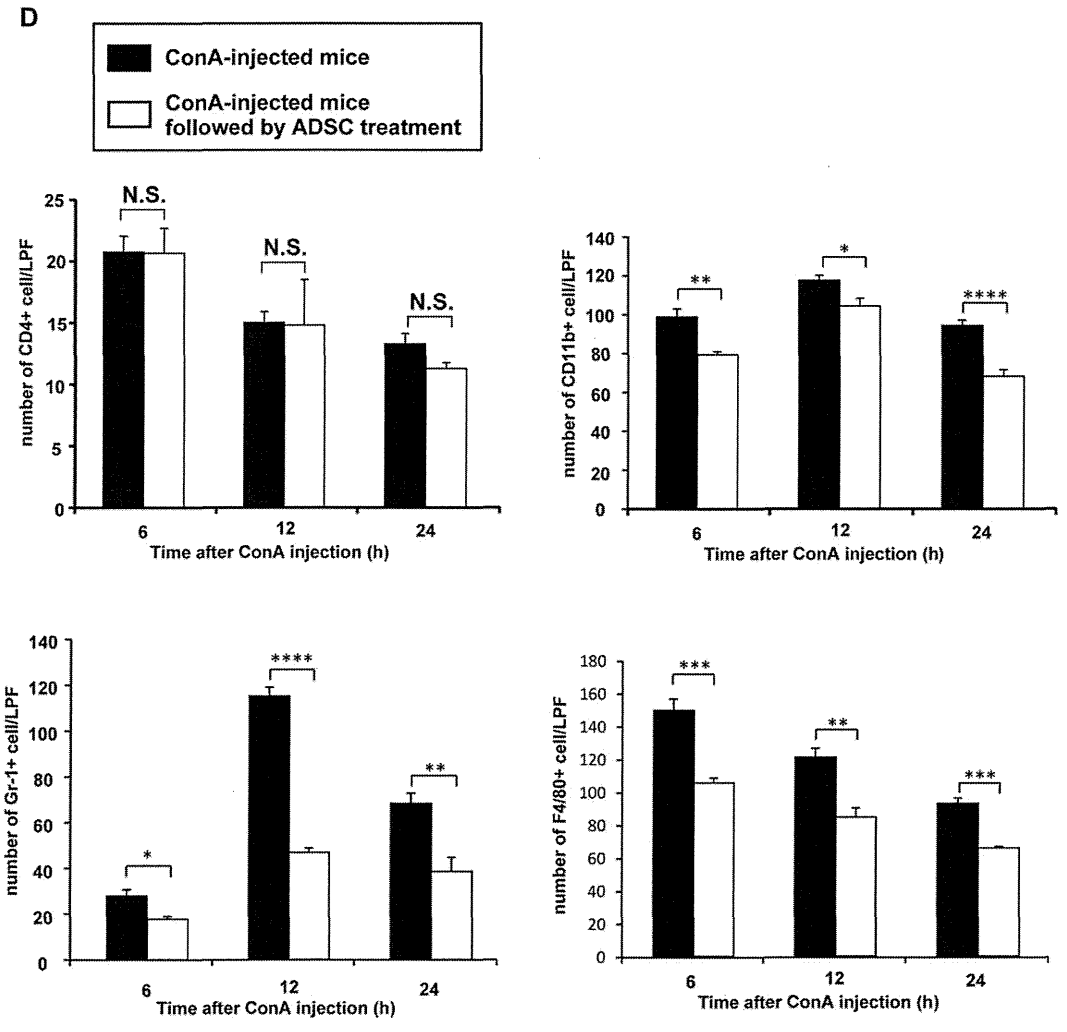

Measurement of serum cytokine/chemokine concentrations

Sera were obtained from ADSC-treated mice immediately or 3 h after ConA injection ($n = 3$ and $n = 4$, respectively), and from ConA-injected mice not treated with ADSCs ($n = 3$ and $n = 6$, respectively) at 6 h. Serum concentrations of cytokines and chemokines were measured using a Multiplex Bead Immunoassays kit, Mouse Cytokine 20-Plex Panel (Invitrogen, Carlsbad, CA, USA), following the manufacturer's protocol. The kit covers FGF-basic, GM-CSF, IFN-γ, IL-1α, IL-1β, IL-2, IL-4, IL-5, IL-6, IL-10, IL-12 (p40/p70), IL-13, IL-17, IP-10(CXCL10), KC, MCP-1, MIG(CXCL9), MIP-1α, TNF-α, and VEGF.

Histological and immunohistochemical analyses of liver and lung tissues

Harvested liver and lung tissues were fixed in 10% formaldehyde, embedded in paraffin, sectioned at 4 μm, and stained with H&E. For immunohistochemical analysis, the liver tissues were embedded in OCT compound (Sakura Finetek, Torrance, CA, USA), snap-frozen in liquid nitrogen, cryostat-sectioned, and fixed with methanol/acetone (1:1). The paraffin-embedded tissues were also sliced into 4 μm sections, mounted on microscope slides, and deparaffinized, followed by epitope retrieval using proteinase K (Dako, Glostrup, Denmark). The slides were incubated with peroxidase blocking reagent (Dako) for 15 min at room temperature to inhibit endogenous peroxidase activity, followed by incubation with protein blocking reagent (Dako) to avoid nonspecific protein reactions. The slides were incubated with primary antibodies (anti-mouse CD4, CD11b, Gr-1, F4/80) (BD Pharmingen, San Diego, CA, USA) and anti-GFP (MBL, Nagoya, Japan) diluted with PBS containing 1% BSA overnight at 4°C. After washing in PBS, the slides were then incubated with secondary antibodies (anti-rat, anti-rabbit; Nichirei, Japan) for 30 min at room temperature. The immune complexes were visualized using EnVision kits /HRP (DAB; Dako) followed by counterstaining with hematoxylin. The numbers of positive cells in each section were counted in four randomly selected fields at 100× magnification under a microscope.

RNA isolation and gene expression analysis by DNA microarray

Total RNA was obtained from the tissues or hepatic inflammatory cells in RNAlater (Ambion) using RNA isolation kit (Sigma-Aldrich) in accordance with the supplied protocol with slight modifications. Isolated RNA was amplified and labeled with the Cy3 using the Quick Amp labeling kit (Agilent Technologies, Santa Clara, CA, USA) in accordance with the manufacturer's protocol. cRNA of 1.65 μg was hybridized onto a Whole Mouse Genome 4 × 44K Array (Agilent Technologies) and scanned using a DNA Microarray Scanner (model G2505B, Agilent Technologies).

Gene expression data were analyzed using the GeneSpring analysis software (Agilent Technologies). Each measurement was divided by the 75th percentile of all measurements in that sample at per chip normalization. Hierarchical clustering and principal component analysis of gene expression was performed. Welch's *t*-test, with Benjamini and Hochberg's false discovery rate, was used to identify genes that were differentially expressed in the groups of interest. Analysis of biological processes was performed using the MetaCore software suite (GeneGo, Carlsbad, CA, USA). BRB array tools (http://linus.nci.nih.gov/BRB-ArrayTools.html) were also used for unsupervised or one-way clustering analyses. Microarray data were deposited in the NBCI Gene Expression Omnibus (GSE ID: GSE41465).

Flow cytometry

Cultured ADSCs were incubated in PBS supplemented with 2% BSA (Sigma-Aldrich) containing antibodies labeled with FITC or PE anti-mouse CD44 or CD90 (Beckman Coulter, Brea, CA, USA), and CD105 (Miltenyi Biotec) antibodies. Hepatic inflammatory cells isolated from mice were incubated with a mixture of FITC-labeled anti-mouse CD204 (AbD Serotec, Raleigh, NC, USA), PE-labeled anti-mouse Gr-1 (Miltenyi Biotec), and allophycocyanin-labeled anti-mouse CD11b (BioLegend, San Diego, CA, USA), or FITC-labeled anti-mouse CD11b (Beckman Coulter), PE-labeled anti-mouse Ly-6G (BioLegend), and allophycocyanin labeled anti-mouse Ly-6C (BioLegend) antibodies. The fluorescence intensity of the cells was measured using a FACSCalibur™ (Becton Dickinson, San Jose, CA, USA). Data obtained were visualized and analyzed using the FlowJo software (Tomy Digital Biology Co., Ltd., Tokyo, Japan).

Isolation of CD11b$^+$Gr-1$^+$ hepatic inflammatory cells and T-cell [3H]-thymidine incorporation assay

C57BL/6J female mice were injected with 300 μg of ConA and then injected with 1×10^5 ADSCs after 3 h ($n = 3$). Three

◀ **Figure 5.** Immunohistochemical analysis of inflammatory cells in the liver of ConA-induced hepatitis mice treated with ADSCs. (A–C) Immunohistochemical staining of the liver. C57BL/6 female mice were injected i.v. with 300 μg of ConA. Then, 3 h later, the mice were injected with ADSCs via the tail vein. Liver tissues were obtained at (A) 6, (B)12, or (C) 24 h after ConA injection ($n = 4$ per each time point). Immunohistochemical staining was conducted using anti-CD4, anti-CD11b, anti-Gr-1, and anti-F4/80 antibodies. Stained liver images shown are representative of three experiments performed. Magnification: ×100. Bars: 200 μm. (D) Quantification of CD4$^+$, CD11b$^+$, Gr-1$^+$, and F4/80$^+$ cells in four visual fields per ×100 low-power field in the liver of representative mice from each group. Data are shown as mean +SE ($n = 4$) and are representative of three experiments performed. $^*p < 0.05$, $^{**}p < 0.01$, $^{***}p < 0.005$, $^{****}p < 0.001$; Student's *t*-test. n.s.: not significant.

hours later, hepatic inflammatory cells were isolated and incubated with FITC-labeled anti-mouse CD11b (Beckman Coulter) and PE-labeled anti-mouse Gr-1 (Miltenyi Biotec) antibodies. The $CD11b^+Gr\text{-}1^+$ population was collected using a FACSAira II™ (Becton Dickinson). $CD11b^+Gr\text{-}1^+$ cells (1×10^5), which had been irradiated with 2000 rads, were co-cultured with 1×10^5 purified splenic T cells isolated from C57BL/6J mice in RPMI1640 medium (Invitrogen) supplemented with 10% heat-inactivated FBS, 1% antibiotic–antimycotic solution (Life Technologies), and ConA (4 μg/mL) for 48 h ($n = 4$). The culture was pulsed with [3H]thymidine (1 μCi/well) for 16 h and harvested. Thymidine incorporation was measured using a beta-counter (PerkinElmer, Waltham, MA, USA).

NO assay

C57BL/6J female mice were injected with 300 μg of ConA. Three hours later, 1×10^5 ADSCs were injected via the tail vein. After a further 3 h, hepatic inflammatory cells were isolated from ConA hepatitis mice with or without ADSC treatment ($n = 3$ each) and incubated in PBS supplemented with 2% BSA, PE-labeled anti-mouse Gr-1 antibody, and allophycocyanin-labeled anti-mouse CD11b antibody. Cells were then incubated in PBS containing 2.5 mg/mL diaminofluorescein-FM diacetate (Sekisui Medical Co., Ltd., Tokyo, Japan), which emits fluorescence at 515 nm in a reaction with NO, at 37°C for 30 min and subjected to FACS analysis using a FACSCalibur flow cytometer.

Arginase assay

Female C57BL/6J mice were injected with 300 μg of ConA. Three hours later, 1×10^5 ADSCs were injected via the tail vein. After further 3 h, hepatic inflammatory cells were isolated from ConA hepatitis mice with or without ADSC treatment ($n = 3$ each) and were lysed with PBS containing 10 mM Tris-HCl (pH 7.4) and 0.4% Triton X-100, supplemented with the proteinase inhibitor cocktail, cOmplete, Mini, EDTA-free® (Roche, Basel, Switzerland). One hundred micrograms of the lysis aliquot obtained were subject to an arginase activity assay using a QuantiChrom™ Arginase Assay kit (BioAssay Systems, Hayward, CA), which measures urea produced from the substrate, in accordance with the manufacturer's protocol.

Statistical analysis

All data are expressed as means ± SE. Statistical analyses were performed using the JMP software (ver.9.02; SAS Institute Japan Inc., Tokyo, Japan). Student's *t*-test and Wilcoxon signed-rank test were used. p values < 0.05 were considered to indicate statistical significance.

Acknowledgements: This study was supported, in part, by subsidies from the Japanese Ministry of Education, Culture, Sports, Science, and Technology and the Japanese Ministry of Health, Labor, and Welfare.

Conflict of interest: The authors declare no financial or commercial conflict of interest.

References

1 **Zuk, P. A., Zhu, M., Ashjian, P., De Ugarte, D. A., Huang, J. I., Mizuno, H., Alfonso, Z. C. et al.**, Human adipose tissue is a source of multipotent stem cells. *Mol. Biol. Cell* 2002. **13**: 4279–4295.

2 **Chamberlain, G., Fox, J., Ashton, B. and Middleton, J.**, Concise review: mesenchymal stem cells: their phenotype, differentiation capacity, immunological features, and potential for homing. *Stem Cells* 2007. **25**: 2739–2749.

3 **Perez-Cano, R., Vranckx, J. J., Lasso, J. M., Calabrese, C., Merck, B., Milstein, A. M., Sassoon, E. et al.**, Prospective trial of adipose-derived regenerative cell (ADRC)-enriched fat grafting for partial mastectomy defects: the RESTORE-2 trial. *Eur. J. Surg. Oncol.* 2012. **38**: 382–389.

4 **Janssens, S.**, Stem cells in the treatment of heart disease. *Annu. Rev. Med.* 2010. **61**: 287–300.

5 **Hoogduijn, M. J., Popp, F., Verbeek, R., Masoodi, M., Nicolaou, A., Baan, C. and Dahlke, M. H.**, The immunomodulatory properties of mesenchymal stem cells and their use for immunotherapy. *Int. Immunopharmacol.* 2010. **10**: 1496–1500.

6 **Baroni, G. S., Pastorelli, A., Manzin, A., Benedetti, A., Marucci, L., Solforosi, L., Di Sario, A. et al.**, Hepatic stellate cell activation and liver fibrosis are associated with necroinflammatory injury and Th1-like response in chronic hepatitis C. *Liver* 1999. **19**: 212–219.

7 **Cerny, A. and Chisari, F. V.**, Pathogenesis of chronic hepatitis C: immunological features of hepatic injury and viral persistence. *Hepatology* 1999. **30**: 595–601.

8 **Gershwin, M. E., Ansari, A. A., Mackay, I. R., Nakanuma, Y., Nishio, A., Rowley, M. J. and Coppel, R. L.**, Primary biliary cirrhosis: an orchestrated immune response against epithelial cells. *Immunol. Rev.* 2000. **174**: 210–225.

9 **Krawitt, E. L.**, Autoimmune hepatitis. *N. Engl. J. Med.* 1996. **334**: 897–903.

10 **Fujii, H. and Kawada, N.**, Inflammation and fibrogenesis in steatohepatitis. *J. Gastroenterol.* 2012. **47**: 215–225.

11 **Dienes, H. P. and Drebber, U.**, Pathology of immune-mediated liver injury. *Dig. Dis.* 2010. **28**: 57–62.

12 **Dai, L. J., Li, H. Y., Guan, L. X., Ritchie, G. and Zhou, J. X.**, The therapeutic potential of bone marrow-derived mesenchymal stem cells on hepatic cirrhosis. *Stem Cell Res.* 2009. **2**: 16–25.

13 **Sanders, D. A., Moothoo, D. N., Raftery, J., Howard, A. J., Helliwell, J. R. and Naismith, J. H.**, The 1.2 A resolution structure of the Con A-dimannose complex. *J. Mol. Biol.* 2001. **310**: 875–884.

14 **Kato, M., Ikeda, N., Matsushita, E., Kaneko, S. and Kobayashi, K.**, Involvement of IL-10, an anti-inflammatory cytokine in murine liver injury induced by concanavalin A. *Hepatol. Res.* 2001. **20**: 232–243.

15 **Kubo, N., Narumi, S., Kijima, H., Mizukami, H., Yagihashi, S., Hakamada, K. and Nakane, A.**, Efficacy of adipose tissue-derived mesenchymal stem cells for fulminant hepatitis in mice induced by concanavalin A. *J. Gastroenterol. Hepatol.* 2012. **27**: 165–172.

16 **Murdoch, C., Muthana, M., Coffelt, S. B. and Lewis, C. E.**, The role of myeloid cells in the promotion of tumour angiogenesis. *Nat. Rev. Cancer* 2008. **8**: 618–631.

17 **Banas, A., Teratani, T., Yamamoto, Y., Tokuhara, M., Takeshita, F., Quinn, G., Okochi, H. et al.**, Adipose tissue-derived mesenchymal stem cells as a source of human hepatocytes. *Hepatology* 2007. **46**: 219–228.

18 **Kaneko, Y., Harada, M., Kawano, T., Yamashita, M., Shibata, Y., Gejyo, F., Nakayama, T. et al.**, Augmentation of Valpha14 NKT cell-mediated cytotoxicity by interleukin 4 in an autocrine mechanism resulting in the development of concanavalin A-induced hepatitis. *J. Exp. Med.* 2000. **191**: 105–114.

19 **Tiegs, G., Hentschel, J. and Wendel, A.**, A T cell-dependent experimental liver injury in mice inducible by concanavalin A. *J. Clin. Invest.* 1992. **90**: 196–203.

20 **Halder, R. C., Aguilera, C., Maricic, I. and Kumar, V.**, Type II NKT cell-mediated anergy induction in type I NKT cells prevents inflammatory liver disease. *J. Clin. Invest.* 2007. **117**: 2302–2312.

21 **Schwabe, R. F. and Brenner, D. A.**, Mechanisms of liver injury. I. TNF-alpha-induced liver injury: role of IKK, JNK, and ROS pathways. *Am. J. Physiol. Gastrointest. Liver Physiol.* 2006. **290**: G583–G589.

22 **Schumann, J., Wolf, D., Pahl, A., Brune, K., Papadopoulos, T., van Rooijen, N. and Tiegs, G.**, Importance of Kupffer cells for T-cell-dependent liver injury in mice. *Am. J. Pathol.* 2000. **157**: 1671–1683.

23 **Clegg, C. H., Rulffes, J. T., Wallace, P. M. and Haugen, H. S.**, Regulation of an extrathymic T-cell development pathway by oncostatin M. *Nature* 1996. **384**: 261–263.

24 **Constant, S. L. and Bottomly, K.**, Induction of Th1 and Th2 CD4+ T cell responses: the alternative approaches. *Annu. Rev. Immunol.* 1997. **15**: 297–322.

25 **Contento, R. L., Molon, B., Boularan, C., Pozzan, T., Manes, S., Marullo, S. and Viola, A.**, CXCR4-CCR5: a couple modulating T cell functions. *Proc. Natl. Acad. Sci. USA* 2008. **105**: 10101–10106.

26 **Ponte, A. L., Marais, E., Gallay, N., Langonne, A., Delorme, B., Herault, O., Charbord, P. et al.**, The in vitro migration capacity of human bone marrow mesenchymal stem cells: comparison of chemokine and growth factor chemotactic activities. *Stem Cells* 2007. **25**: 1737–1745.

27 **Kushiyama, T., Oda, T., Yamada, M., Higashi, K., Yamamoto, K., Oshima, N., Sakurai, Y. et al.**, Effects of liposome-encapsulated clodronate on chlorhexidine gluconate-induced peritoneal fibrosis in rats. *Nephrol. Dial. Transplant.* 2011. **26**: 3143–3154.

Abbreviations: **ADSC:** adipose tissue derived stromal stem cell · **ALT:** alanine transferase · **LDH:** lactate dehydrogenase · **MDSC:** myeloid-derived suppressor cell · **MSC:** mesenchymal stromal stem cell

Full correspondence: Dr. Shuichi Kaneko, Disease Control and Homeostasis, Kanazawa University, 13-1 Takara-machi, Kanazawa, Ishikawa 920-8641, Japan
Fax: +81-76-234-4250
e-mail: skaneko@m-kanazwa.jp

Received: 17/3/2013
Revised: 3/7/2013
Accepted: 6/8/2013
Accepted article online: 12/8/2013

HEPATOLOGY
Official Journal of the American Association for the Study of Liver Diseases

LIVER INJURY/REGENERATION

Adipose Tissue-Derived Stem Cells as a Regenerative Therapy for a Mouse Steatohepatitis-Induced Cirrhosis Model

Akihiro Seki,[1,2*] Yoshio Sakai,[1,3*] Takuya Komura,[2] Alessandro Nasti,[2] Keiko Yoshida,[2] Mami Higashimoto,[2] Masao Honda,[1] Soichiro Usui,[2] Masayuki Takamura,[2] Toshinari Takamura,[2] Takahiro Ochiya,[4] Kengo Furuichi,[5] Takashi Wada,[3] and Shuichi Kaneko[1,2]

Cirrhosis is a chronic liver disease that impairs hepatic function and causes advanced fibrosis. Mesenchymal stem cells have gained recent popularity as a regenerative therapy since they possess immunomodulatory functions. We found that injected adipose tissue-derived stem cells (ADSCs) reside in the liver. Injection of ADSCs also restores albumin expression in hepatic parenchymal cells and ameliorates fibrosis in a nonalcoholic steatohepatitis model of cirrhosis in mice. Gene expression analysis of the liver identifies up- and down-regulation of genes, indicating regeneration/repair and anti-inflammatory processes following ADSC injection. ADSC treatment also decreases the number of intrahepatic infiltrating CD11b$^+$ and Gr-1$^+$ cells and reduces the ratio of CD8$^+$/CD4$^+$ cells in hepatic inflammatory cells. This is consistent with down-regulation of genes in hepatic inflammatory cells related to antigen presentation and helper T-cell activation. *Conclusion*: These results suggest that ADSC therapy is beneficial in cirrhosis, as it can repair and restore the function of the impaired liver. (HEPATOLOGY 2013;58:1133-1142)

Cirrhosis is a serious, life-threatening advanced stage of chronic liver disease that leads to hepatic dysfunction.[1] Cirrhosis frequently develops into hepatocellular carcinoma,[2,3] which exacerbates the prognosis of patients with cirrhosis. The ultimate treatment for cirrhosis is a liver transplant,[4] which can be lethal.[5] The number of donor livers, however, is not sufficient to meet the needs of all transplant patients. Thus, a novel therapy for cirrhosis needs to be developed to improve cirrhotic liver prognosis.

The underlying pathogenesis of chronic liver disease is persistent inflammation. Advanced disease is marked by advanced fibrosis concomitant with distorted liver architecture characterized by regenerative nodules and impaired hepatic function. Advanced fibrosis in the cirrhotic liver is also a risk factor for the development of hepatocellular carcinoma.[6] Treatment of cirrhosis suppresses inflammation by eradicating hepatitis virus infection or reducing liver steatosis in nonalcoholic steatohepatitis (NASH). Decreasing liver inflammation and restoring hepatocyte function improves the prognosis.

Pluripotent mesenchymal stem cells (MSCs) differentiate into adipocyte, chondrocyte, and osteocyte lineages.[7] These cells can also differentiate into other lineages, including neurons[8] and hepatocytes.[9,10] MSCs can also regulate the immune response.[11] Thus, MSCs attract attention as a therapeutic target in the

Abbreviations: ADSCs, adipose-tissue-derived stem cells; AFP, alpha-fetoprotein; Ath+HF, atherogenic high-fat; IL, interleukin; MMP, matrix metalloproteinase; MSC, mesenchymal stem cells; NASH, nonalcoholic steatohepatitis; PBS, phosphate-buffered saline; 18S rRNA, 18S ribosomal RNA; α-SMA, alpha-smooth muscle actin.

From the [1]Department of Gastroenterology, Kanazawa University Hospital, Ishikawa, Japan; [2]Disease Control and Homeostasis, Kanazawa University, Ishikawa, Japan; [3]Department of Laboratory Medicine, Kanazawa University Hospital, Ishikawa, Japan; [4]National Cancer Research Institute, Tokyo, Japan; [5]Division of Blood Purification, Kanazawa University Hospital, Ishikawa, Japan.

Received September 27, 2012; accepted April 15, 2013.

Supported in part by subsidies from the Japanese Ministry of Education, Culture, Sports, Science and Technology and the Japanese Ministry of Health, Labor and Welfare.

**These authors contributed equally to this work.*

regeneration or repair of various impaired organs. Mesenchymal tissue from bone marrow, umbilical cord, and adipose tissue are relatively enriched with pluripotent stem cells.[12] Since the pathophysiological features of liver cirrhosis are a consequence of chronic hepatic inflammation, MSCs are especially suited to enhance regeneration and/or repair of damaged cirrhotic liver.

We have established a clinically relevant NASH cirrhotic murine model by feeding animals an atherogenic high-fat (Ath+HF) diet.[13] In this study we examined whether adipose-tissue-derived stem cells (ADSCs) can regenerate and/or repair the cirrhotic liver. We observed that injected ADSCs resided in the liver and expressed albumin, leading to restored albumin expression in hepatic parenchymal cells. ADSCs also ameliorated advanced fibrosis. Moreover, ADSCs suppressed the underlying persistent inflammation contributed by granulocytes, phagocytic cells, and T cells. These results suggest that treatment of patients with cirrhosis with ADSCs is a potentially novel approach for regenerating and/or repairing damaged cirrhotic liver tissue to restore hepatic function.

Materials and Methods

Culture of ADSCs. ADSCs were prepared as described.[14] Briefly, adipose tissue was obtained from the inguinal subcutaneous region of 10-week-old GFP-Tg male mice (a gift from Professor Okabe, Osaka University, Japan). The stem cell fraction was isolated from adipose tissue using type-I collagenase (Wako Pure Chemical Industries, Osaka, Japan) and cultured in Dulbecco's modified Eagle's medium: nutrient mixture F-12 supplemented with 10% heat-inactivated bovine serum albumin and 1% antibiotic-antimycotic solution. Cell culture reagents were purchased from Life Technologies (Carlsbad, CA).

NASH Murine Model. Female 8-week-old C57Bl/6J mice were purchased from Charles River Laboratories Japan (Yokohama, Japan). Mice were fed an Ath+HF diet composed of cocoa butter, cholesterol, cholate, and corticotropin-releasing factor-1 (Oriental Yeast Co., Tokyo, Japan) to induce steatohepatitis as reported previously.[13] Our Institutional Review Board approved the care and use of laboratory animals in all experiments.

ADSC Treatment of NASH Mice. ADSCs were harvested after six to eight passages in culture by treatment with trypsin/EDTA (Life Technologies) and passed through a 100-μm Cell Strainer mesh (BD Biosciences, San Jose, CA). Laparotomy was performed to inject 1×10^5 ADSCs or phosphate-buffered saline (PBS) into the splenic subcapsule. After ADSC treatment, the mice were anesthetized with pentobarbital (40 mg/kg; Kyoritsu Seiyaku, Tokyo, Japan), after which the liver was perfused with PBS and dissected. A portion of liver tissue was homogenized and incubated with type I collagenase (Wako Pure Chemical Industries), and hepatic parenchymal cells and inflammatory cells were separated with Percoll (GE Healthcare UK, Buckinghamshire, UK). $CD4^+$ T cells were isolated from hepatic inflammatory cells using a magnetic sorting system, the $CD4^+$ T cell Isolation Kit II (Miltenyi Biotec, Gladbach, Germany).

Histology and Immunohistochemical Staining. Liver tissue was preserved with formalin for paraffin embedding or embedded in OCT compound and frozen for sectioning (Sakura Finetek Japan, Tokyo, Japan). The frozen liver sections were fixed in acetone and endogenous peroxidase activity blocked with 3% hydrogen peroxide solution. After washing in PBS, the sections were incubated with a rabbit anti-CD11b antibody (BD Pharmingen, San Diego, CA) and a rabbit anti-Gr-1 antibody (eBioscience, San Diego, CA) overnight at 4°C. The slides were then washed and incubated with Histofine mouse MAXPO (Nichirei Bioscience, Tokyo, Japan) for 1 hour at room temperature. The immune complex was visualized by incubating with diaminobenzidine for 5 minutes. The paraffin-embedded sections were stained with a rabbit-anti-GFP antibody (Millipore, Billerica, MA), a rabbit anti-α-smooth muscle actin (α-SMA) antibody (Abcam, Cambridge, UK), and a rabbit anticollagen IV antibody (Abcam). Secondary antibody development was performed with diaminobenzidine as described above. In some experiments, the sliced

Address reprint requests to: Shuichi Kaneko, 13-1 Takara-machi, Kanazawa, Ishikawa 920-8641, Japan. E-mail: skaneko@m-kanazawa.jp; fax: +81-76-234-4250.

View this article online at wileyonlinelibrary.com.
DOI 10.1002/hep.26470
Potential conflict of interest: Nothing to report.
Additional Supporting Information may be found in the online version of this article.